REPUBLIC OF TÜRKİYE

ALTINBAŞ UNIVERSITY

Institute of Graduate Studies

Mechanical Engineering

NUMERICAL INVESTIGATION OF TWO-PHASE FLOW CHARACTERISTICS IN CENTRIFUGAL PUMPS

Osamah Najah Mubark KWESHE

Master's Thesis

Supervisor

Asst. Prof. Dr. Yaser ALAIWI

İstanbul, 2024

NUMERICAL INVESTIGATION OF TWO-PHASE FLOW CHARACTERISTICS IN CENTRIFUGAL PUMPS

Osamah Najah Mubark KWESHE

Mechanical Engineering

Master's Thesis

ALTINBAŞ UNIVERSITY

2024

This thesis title NUMERICAL INVESTIGATION OF TWO-PHASE FLOW CHARACTERISTICE IN CENTRIFUGAL PUMPS prepared by OSAMAH NAJAH MUBARK KWESHE and submitted on 09/01/2024 has been **accepted unanimously** for the degree of Master of Science in Mechanical Engineering.

____

Asst. Prof. Dr. Yaser ALAIWI

Signature

Thesis Defense Committee Members:

Asst. Prof. Dr. Yaser ALAIWI	Department of Mechanical Engineering, Altınbaş University	_________________
Asst. Prof. Dr. Abdullahi Abdu IBRAHIM	Department of Computer Engineering, Altınbaş University	_________________
Asst. Prof. Dr. Haydar İzzettin KEPEKÇI	Department of Mechatronics Engineering, İstanbul Gelişim University	_________________

I hereby declare that this thesis meets all format and submission requirements of a Master's thesis.

I hereby declare that all information/data presented in this graduation project has been obtained in full accordance with academic rules and ethical conduct. I also declare all unoriginal materials and conclusions have been cited in the text and all references mentioned in the Reference List have been cited in the text, and vice versa as required by the abovementioned rules and conduct.

Osamah Najah Mubark KWESHE

Signature

PREFACE

I'd like to express my appreciation to my advisor, Asst. Prof. Dr. Yaser ALAIWI, and dedicate this research to him for his dedication to establishing a sound scientific methodology through our many productive discussions. for his meticulous follow-up on this study effort and to all my friends and family who have been so supportive. In addition, I'd like to thank the distinguished members of my faculty and the department head for the crucial roles they play, as well as everyone who has helped make this institution the outstanding center of learning that it is today.

ABSTRACT

NUMERICAL INVESTIGATION OF TWO-PHASE FLOW CHARACTERISTICS IN CENTRIFUGAL PUMPS

KWESHE, Osamah Najah Mubark
M.Sc., Mechanical Engineering, Altınbas University,
Supervisor: Asst. Prof. Dr. Yaser ALAIWI
Date: January / 2024
Pages: 57

Due to its important applications, particularly in the oil and gas industry, two-phase pumping has been the subject of several studies. This study includes a numerical investigation of two-phase flow inside a centrifugal impeller with seven blades, at a rotational speed of 2500 rpm and an inlet pressure of 100000 Pa. The simulation includes investigating the effect of flow rate, gas volume fraction GVF, and bubble sizes on the pump performance curves and also on the phase distribution through the impeller. Four flow rate values of 2.4, 3.1, 3.9, and 4.6 kg/s, four GVF values of 0.1, 0.15, 0.2, and 0.3, and four bubble sizes of 0.1, 0.2, 0.3, and 0.5 mm are considered in the simulation. The governing equation and the turbulent kinetic energy dissipation (k - ε) model are solved using ANSYS software.

The results show that increasing the flow rate leads to a decrease in the pump head and hydraulic efficiency under single- and two-phase operations, with reduced performance in the case of the two-phase condition. The head and efficiency are also significantly affected by increasing the GVF and bubble diameter. Increasing the GVF from 0.1 to 0.3 causes the head to decrease by about 26% and hydraulic efficiency by up to 25%. The impact of bubble size, on the other hand, depends on the flow rate and bubble diameter. A significant reduction in pump performance by increasing bubble diameter has been reported for low flow rates, while only a limited impact has been observed for high flow rates, particularly at large bubble sizes. Gas pocket formation has been visualized at the inlet upper pressure side of the impeller blade in cases of high GVF and bubble diameters.

Keywords: Phase Flow, CFD, Centrifugal Pump, Bubble Sizes, Gas–Liquid.

TABLE OF CONTENTS

LIST OF TABLES

Pages

LIST OF FIGURES

Pages

ABBREVIATIONS

CFD	:	Computational Fluid Dynamic
VOF	:	Volume of Fluid
FVM	:	Finite Volume Method
NS	:	Navier–Stokes
EVM	:	Eddy Viscosity Models
GVF	:	Gas Volume Fraction

LIST OF SYMBOLS

k	:	Turbulent Kinetic Energy
μ_t	:	Eddy Viscosity
d_p	:	Diameter of the Bubbles
H	:	Head
Q	:	Flow Rate
P	:	Pressure
α_q	:	Volume Fraction Phase
$\vec{F}_q$	:	External Body Force
$\vec{V}_{pq}$	:	Interphase Velocities
f	:	Drag Function
C_l	:	Lift Force Coefficient

1. INTRODUCTION

1.1 GENERAL BACKGROUND

From a long time ago until now, there has been a continuous need to lift the fluids from one level to higher levels. Over time, pumps have been considered one of the most important and widely used mechanical lift methods around the world. Indeed, it has been reported that pumps are the second most common mechanical device, coming directly after electric motors [1]. A pump is a hydromechanical unit that increases the hydraulic energy of the fluid being pumped. The early pumps were large and heavy, driven manually or by animal power, and used for limited purposes, mainly for supplying water and irrigation. Today, the pumps maintain the same basic principle but have totally changed in shape, size, and driving method [2]. Furthermore, pump applications have greatly expanded to include various practical and industrial applications, such as water supply, irrigation, the chemical industry, the petroleum industry, and others [3].

Based on their working principle, pumps are either positive displacement or dynamic [4]. The prime difference between the two types is that while positive displacement pumps provide a specific fluid volume in a specific time interval, dynamic pumps provide continuous fluid discharge [5]. However, for applications with medium and high flow rates, dynamic pumps are the only correct selection. The dynamics pumps can be divided into centrifugal pumps and special effect pumps [6],[7]. The centrifugal pump is the most frequently used type of pump due to its superior advantages. The centrifugal pump is simple in design, its reliability and efficiency are high [8], it is economical in operation and maintenance, and it can be operated with most fluids at different flow rates and heads. It is worth mentioning that 80–90% of the pumps installed in a typical petroleum plant are centrifugal [9].

A centrifugal pump is characterized by an impeller that rotates inside a casing , as seen in Figure 1.1. The fluid is drawn to the rotating impeller through the casing eye, where it accelerates and gains velocity due to the centrifugal forces exerted on the fluid by the impeller, then leaves through the diffuser section (volute). The kinetic energy is changed into pressure energy by passing it through the impeller blades and then again by passing it through the diffuser or the volute section of the casing. [10].

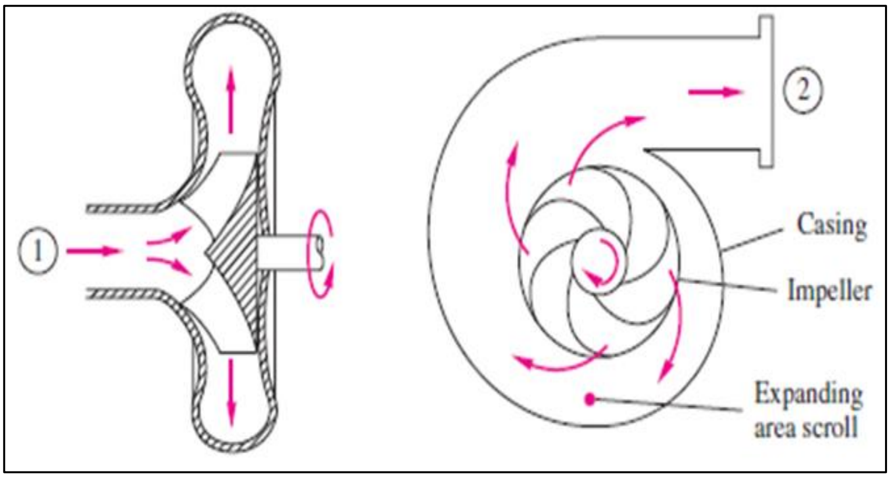

Figure 1.1: Schematic of a Typical Centrifugal Pump [10].

Centrifugal pumps come in various types and can be categorized into several methods. Based on the orientation of the pump shaft axis, they are horizontal or vertical, as shown in Figure 1.2. Based on the number of stages, they can be single-stage or multi stages pumps. The multistage pump, demonstrated in Figure 1.3, is used to produce high pressure. Every single stage provides a specific pressure, and the total pump pressure is almost equal to the stage pressure multiplied by the number of stages [9]. The submersible pump is a particular type of centrifugal pump, used to extract fluids from deep wells. It is commonly a vertical, multistage centrifugal pump, with each stage consisting of an impeller followed by a diffuser in order to increase the pressure and secure the flow smoothness between the pump stages [11],[12]. Figure 1.4 shows this type of pump with the main components.

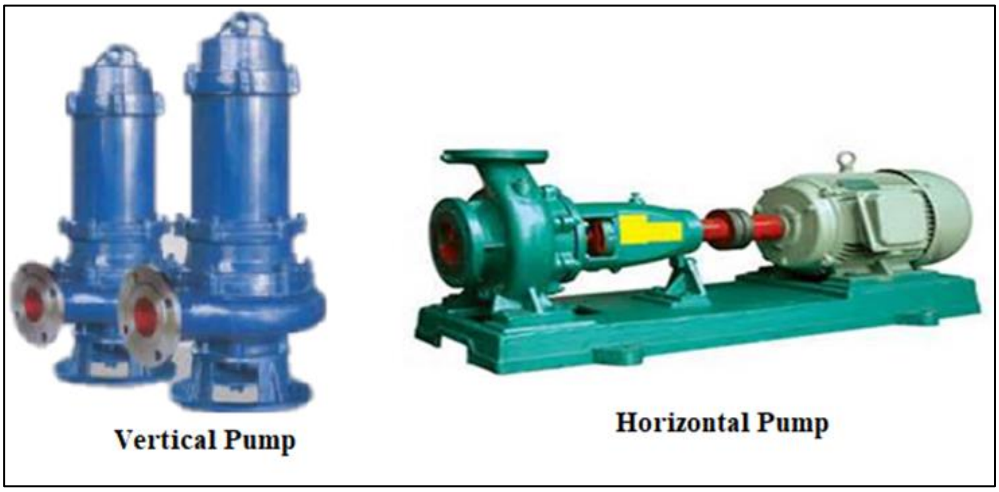

Figure 1.2: Horizontal and Vertical Pumps [13].

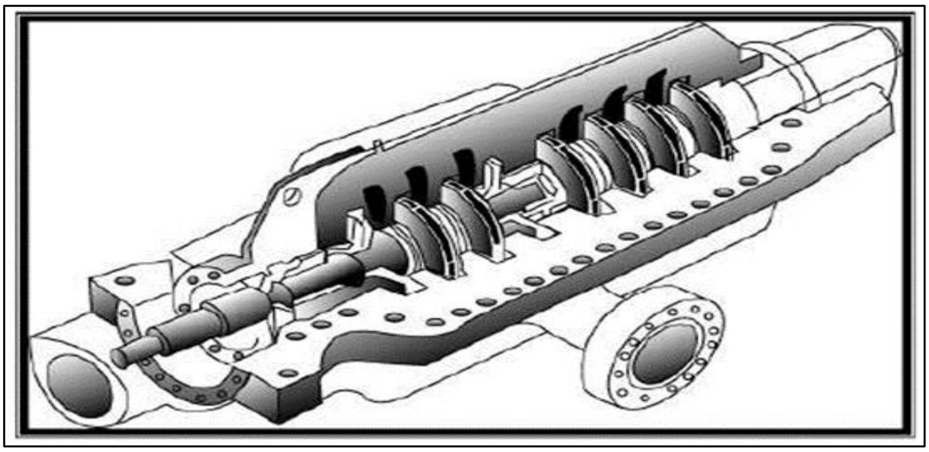

Figure 1.3: Multistage Pump[13].

Figure 1.4: Submersible Pumps [13].

The centrifugal pumps require being driven by a prime mover, including an electrical motor, an internal combustion engine, and steam or gas turbines. The selection of the optimal driving motor depends on many factors, including the application, the availability, the running and maintenance costs, and the speed control [3].

Although the construction of the centrifugal pump is simple, an impeller rotates in a casing, and the flow through it is very complex. The flow is typically three-dimensional, unsteady, and turbulent [14]. This fact is true even in a single-phase flow, and the situation becomes more complex in two-phase flows. To enhance the efficiency of the centrifugal pump operation, it is crucial to have a comprehensive grasp of the flow dynamics within the pump components. particularly through the impeller [15],[16]. Four main secondary flow structures were demonstrated within the impeller only as a result of the combined effects of normal, axial, and rotational flows in the presence of blade curvature and rotational force effects [17].Furthermore, the centrifugal pumps require being driven by a prime mover, including an electrical motor, an internal combustion engine, and steam or gas turbines.

Therefore, it is necessary for the study to consider the properties of the turbulent boundary layer as well as the impacts of mixing on the turbulent kinetic energy, dissipation rates, and losses [18]. The flow unsteadiness phenomena in centrifugal pumps, such as rotating stall, impeller-volute (or diffuser) interaction, and reverse currents, can lead to pressure pulsation and flow instability, particularly in off-design operations [15], [12].

Two-phase flows can be frequently encountered in the gas and oil industries, where a slight fraction of gas can be encountered in the oil [19]. Hence, pumps that are utilized to operate in these industries have to handle such liquid-gas flows in some situations. Multiphase pumping may be associated with some problems, such as deviation from the nominated operation point or even total failure of the process as a result of vapor locking [20]. Furthermore, in rotary pumps, these two phases, the liquid, and the gas, are separated because there is a significant difference in their physical properties [21]. The gas phase is expected to gather on the impeller core and blade inlet surfaces, resulting in reduced efficiency for the entire pump. More importantly, the pressure pulsation that happens if the gas volume percentage reaches a specific threshold has a direct impact on the stabilization of multiphase pump performance [22],[23]. Indeed, it has been proven that the efficiency of the pumps is significantly lower when delivering multi-phase fluids in comparison to single-phase fluids. The level at which efficiency and performance fall depends on various parameters, including gas volume fraction, flow properties and patterns, impeller, and volute (or diffuser) geometries, and pump speed [24].

The existing flow patterns determine the categorization of two-phase flow into different types or modes. The structure of the flow pattern is determined by the phase fractions, the flow velocity, and the geometry's shape and orientation [25],[26]. For horizontal pipe, for example, the two-phase flow modes and map are demonstrated in Figure 1.5. In the separated flows, there are distinct borders between the two phases. For example, in stratified flow, one phase flows above the other without any mixing between them. Also, in the annular flow, the liquid film flows along the tube surfaces, and the gas phase flows in the middle. On the other hand, in inhomogeneous flows, one phase is dispersed throughout the flow as discrete particles or bubbles, while the other phase is continuous, as can be seen in the bubble flow [27],[28]. However, there is some system that includes both separated and homogeneous bubbly flow , such as the annular bubble flow. In fact, because of the increasing instability in any mode, it is possible to be transferred from one flow pattern to another at any time. This makes the simulation of the two-phase flows very complicated, as this phenomenon is unpredictable [29].

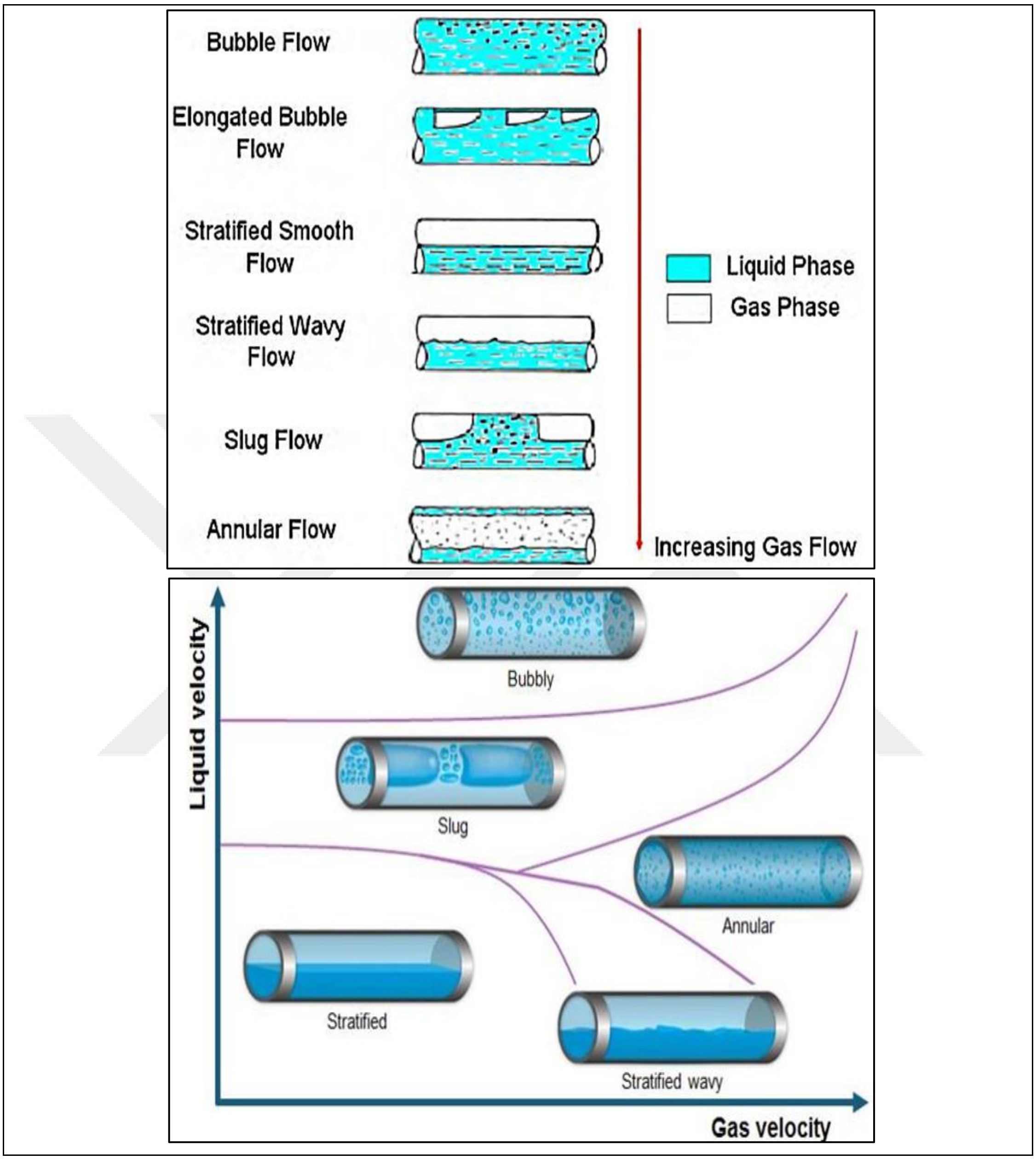

Figure 1.5: Two-Phase Flow Patterns and Maps in A Horizontal Tube [29].

The performance of two-phase pumping has been considered by many researchers, who have tried to discuss and explain the associated physical characteristics to clarify the matter [30]. In 1978, Patel and Rund Stadler presented an analysis of the pump's performance when a small fraction of air was introduced to the pump inlet; hence, a flow of a mixture of water and air exists. They stated that because of the low density of the air compared to the water density, when comparing the air and water phases, you will observe a difference in velocity, and the flow pattern is bubbly[31]. When the velocity differences grow and become large enough, the bubbles merge, resulting in the formation of a large void, which is the fraction of air relative to water. Then, as a result, the bubbly flow converts to a separated flow [32]. In addition, the gas volume fraction goes all the way from the blade's entry to its exit when you look at the flow through the turbine. The density of both the gas and liquid phases will have an impact on the pump head rather than just the density of the liquid phase. Which means that when two-phase pumping happens, the pump head will go down [33]. Further, the gas phase will decrease the propeller passage cross-section, speed up the water, and lower the pump head even more [32],[34].

The pump's performance in two-phase flows is highly contingent upon the flow pattern at the pump's inlet. The flow pattern is assumed to be bubbly and homogeneous based on analytical and experimental investigations [35]. However, there is no guarantee that this is always the case, and some kind of flow visualization has to be carried out to identify the real flow pattern [34]. Computational analysis using CFD codes provides powerful tools to demonstrate the flow fields and present a detailed view of the existing situation.

Significant progress has been made in the development of CFD codes during the latter half of the 20th century, and they are now used to solve different engineering problems. The rapid and great development in the computer industry has contributed to spreading the usage of CFD codes in different engineering applications. For single-phase flows, CFD commercial packages have provided an effective and trustworthy method for solving and analyzing the problem for a long time. Recently, because of the availability of great computational resources and the introduction of several flow models, including those of two-phase flows, into the developed packages, CFD investigations have become essential in such studies [36].

1.2 THE SIGNIFICANCE OF COMPREHENDING THE FEATURES OF TWO-PHASE FLOW FOR THE PURPOSE OF OPTIMIZING PUMP DESIGN AND OPERATION

Understanding two-phase flow characteristics is crucial for the efficient design and operation of pumps, particularly centrifugal pumps, due to several significant reasons [37],[38]:

a. Performance Optimization: Two-phase flow significantly alters the performance of pumps compared to single-phase flow. Accurate knowledge of the behavior of gas-liquid or liquid-liquid mixtures inside the pump allows for the optimization of pump designs to enhance efficiency, reduce energy consumption, and increase reliability.
b. Prevention of Cavitation: Cavitation is a common occurrence in two-phase flows when pressure changes within the pump result in the creation of vapor bubbles. Pump components can be damaged, performance can be reduced, and noise can be generated as a result of cavitation. Gaining a comprehensive understanding of the factors that contribute to cavitation is essential in order to proactively prevent its onset and minimize its detrimental consequences [39].
c. Efficient Material Handling: Certain industries deal with slurries, emulsions, or multiphase fluids where solid particles or immiscible liquids are present. When you fully understand two-phase flow, you can choose the right materials for pump parts that can withstand the wear, erosion, or corrosion that comes from fluids that contain mix of phases. Consequently, this prolongs the operational lifespan of the pump.
d. Prediction of Pump Performance: Two-phase flow significantly alters the performance of pumps compared to single-phase flow. A precise understanding of the dynamics of gas-liquid or liquid-liquid combinations within the pump enables the fine-tuning of pump designs to improve efficiency, minimize energy usage, and boost dependability.
e. Industrial Applications: Many sectors, including oil and gas production, chemical manufacturing, the food and beverage industry, and water purification, frequently handle two-phase fluids. Understanding the behavior of these complex fluid systems within centrifugal pumps is critical for optimizing processes, ensuring safety, and maintaining product quality.
f. Environmental Impact and Energy Efficiency: Improving pump efficiency has direct implications for energy consumption and environmental sustainability. Understanding two-phase flow characteristics aids in developing pumps that operate more efficiently, reducing energy usage, and subsequently minimizing the carbon footprint of industrial processes [40].
g. Safety and Reliability: Operating pumps under two-phase flow conditions requires a thorough understanding to maintain operational safety and reliability. Ensuring the

safety of equipment and people requires the avoidance of concerns such as flow instabilities, pressure surges, or unanticipated system behaviors [41],[42].

h. In conclusion, comprehending the intricacies of two-phase flow within centrifugal pumps is essential for optimizing their design, ensuring efficient operation, reducing maintenance costs, and enhancing overall performance across various industries. This understanding plays a pivotal role in advancing technology and promoting sustainable practices in fluid handling systems.

1.3 RESEARCH PROBLEM

Nowadays, due to the increasing demand for oil and gas resources, any improvement in the efficiency of the extraction and distribution operations will have a significant positive impact on the profits of the companies operating in these industries. Centrifugal pumps are an attractive pumping tool because of their outstanding advantages. The development of using these pumps to deliver two-phase flows while maintaining their high efficiency and reliability would be very beneficial.

The complexity of the phenomenon of two-phase flow makes the analytical solution of the governing equations almost impossible. There are many experimental studies in this area. However, the high cost, the long measurement time, and the limitations of obtaining detailed flow behavior views have led to the use of numerical studies of the two-phase flow problems. Commercial CFD packages can provide very useful tools to demonstrate the detailed flow patterns and their variation as a function of different geometrical and operational parameters of pumping. This helps in understanding the pumping operation and, hence, will lead to developing methods to increase the efficiency of the process.

However, the modeling and simulation of two-phase flow behavior within pumps remain challenging and unresolved. A knowledge gap exists in this area that requires attention. Consequently, the exploration of flow patterns and the factors influencing centrifugal pump performance continues to be of significant interest to researchers.

1.4 THESIS OBJECTIVES

Significant endeavors have been undertaken to create models and simulate the efficiency of centrifugal pumps when operating in two-phase flow circumstances. However, due to its complexity, the phenomenon is not fully understood yet, and further research is required in this field. The present work entails a quantitative examination of the biphasic flow within a centrifugal pump utilizing ANSYS software. The objective of this investigation is to ascertain the flow patterns and bubble dynamics within the pump during two-phase flow while considering various operational situations. Additionally, we seek to establish a correlation between these factors and the pump's performance prediction.

1.5 THESIS OUTLINES

In Chapter Two, following this chapter, a review of the relevant studies concerned with two-phase flow pumping is presented and discussed. Although this study is numerical, experimental, and analytical studies will also be presented for a better understanding of the problem. However, the main focus will be on the CFD analysis studies.

Chapter Three provides an elaborate exposition of the instruments and methodologies employed in the research. The methodology of the CFD programs will be explained, and the governing equations and the turbulence modeling equations for the two-phase flow will be presented and discussed. The pump geometry will be modelled, the boundary conditions will be introduced, and the two-phase flow through the pump will be simulated. A validation study of the pre-obtained results will be carried out by comparing them with the relevant experimental data prior to the main numerical results.

The simulation results produced for the various scenarios are given and analyzed in Chapter 4.The flow patterns through the centrifugal pumps will be demonstrated and discussed. The geometrical and flow factors that affect how well the pump works will be looked at, and the results will be fully explained and talked over.

Finally, in Chapter Five, the overall results will be summarized, and the important conclusion will be presented briefly. Also, some suggestions for future work will be offered in this chapter.

2. LITERATURE REVIEW

2.1 INTRODUCTION

Given its significance and extensive array of practical uses, considerable research has considered two-phase flow through centrifugal pumps. In this review, the most important and relevant aspects of the current study will be presented and analyzed. Although this study is a numerical one using commercial CFD software, the review will also include experimental, visualization, and analytical investigations for a better understanding of the problem under study. However, the most attention in this chapter will go to numerical research.

The investigation of the dynamics of two-phase flow in centrifugal pumps has gained significant attention due to their extensive application in industry, commerce, and science. This review highlights the physics that govern the pump's liquid-gas interaction by selecting the most important results from the wide literature. While numerical simulations are the main method for this study, this review purposefully covers a wider range of investigative methods. Experimental experiments have helped us comprehend two-phase flow using centrifugal pumps by offering real and factual insights. Visualization tools have also helped reveal flow patterns and complex hydrodynamics. The review also considers analytical methods used to gain fundamental insights from two-phase flow equations. This analytical perspective complements the numerical results and provides a theoretical foundation for understanding the phenomenon.

This comprehensive overview emphasizes numerical research due to its importance in the current investigation. Researchers may precisely simulate and evaluate centrifugal pump flow patterns and behavior using modern CFD commercial software. Quantitative data from numerical investigations based on fluid dynamics and thermodynamics helps explain two-phase flow mechanics.

This review explores centrifugal pump two-phase flow in conclusion. The phenomenon is understood holistically by combining numerical, experimental, visualization, and analytical investigations. This holistic approach improves the study's methods and adds to scholarly discourse on centrifugal pump fluid flow dynamics.

2.2 BACKGROUND

The study conducted by Murakami and Minemura [43] was an influential early experimental investigation that specifically examined the performance of centrifugal pumps in two-phase flow settings. They conducted a series of experiments regarding to get a better understanding of how the two-phase pumping effectiveness was affected by the bubble flow as well as the number of blades on the impeller. The results showed that the air bubbles follow a similar streamline as water, and hence they could be used in the flow visualization experiments. The amount of air volume fraction had an effect on the performance of the pump in a way that was dependent on the quantity of impeller blades [44]. Increasing the air volume resulted in a continual decline in the performance of the pump, provided that the number of blades was sufficient (seven in the studies). On the other hand, the efficiency of the pump increased as a result of strengthening the flow pattern through the impeller when there were a small number of blades (three in the investigation) and a small amount of air [45]. This was the case when the experiment was conducted.

Izturiz and Kenyery [46] conducted experimental work to study the effect of the bubble size at the suction section of an electric submersible pump on its performance under air-water flow conditions. The obtained experimental data included the bubble sizes and diameters, pressure and temperature profiles, and performance curves as a function of suction pressure and air volume fraction at various working conditions. It was shown that the bubbles became smaller as they moved inside the consecutive stages as a result of increasing pressure and hence the compressibility impact. Furthermore, the results showed that the suction pressure and air volume fraction have a considerable effect on the pump head and performance. Two-phase flow conditions corresponded to a larger head reduction compared to single-phase pumping under the same circumstances. Also, two-phase flow pumping is characterized by other negative features, including regions of instability and pressure pulsations. The temperature variation did not have any significant effect on the pump characteristics at all operating conditions.

Noghrehkar et al. [47] performed experiments and employed an analytical model to forecast the deterioration of the pump head in a two-phase system. They also examined the interplay between the gas and the fluid within the pump's impeller. The study was conducted in high-pressure settings, namely in a two-phase steam-water flow. Comparing the obtained analytical results with the relevant experimental measurements showed almost identical results, and hence it was concluded that the developed model could predict the phenomenon successfully. The experimental and analytical results demonstrated that for small suction void fractions, the vapor phase totally condensed, and the pump head increased. Conversely, for high suction void fractions, the vapor condensation was partial, and the pump head decreased. Furthermore, the experimental and developed model displayed that for systems of high temperature and/or pressure, the reduction in the pump head was less compared to normal operation. The researchers explained this behavior as a result of the increase in condensation rate in such systems. Many researchers examined the two-phase flow patterns behavior by carrying out visualization experiments at different flow conditions. Amoresano et al. [48] developed a test rig for the centrifugal pump with a transparent casing to observe the flow through it and understand the flow patterns inside the impeller. They used a high-resolution CCD camera and an electrically balanced motor to capture the flow fields and also quantify the energy dissipation phenomenon. The results indicated that the bubble concentration was higher in regions of high pressure near the blades of the impeller. This distribution could cause a change in the pump's characteristics.

Barrios and Prado [49] experimentally visualized the two-phase flow patterns inside one stage of an electrical multistage submersible pump. The dynamic behavior of the flow has been exhibited, and the bubble sizes have been measured using some special high-speed instrumentation in order to assess the pump's performance under different working conditions. They started their experiments by analyzing single-phase flow inside the centrifugal pump and determining the proper rotational speed for the two-phase pumping experiments. For the two-phase flow, the structure of the flow was observed for different liquid flow rates and different pump speeds. The results demonstrated the occurrence of the surging phenomenon, which is an unexpected drop in the magnitude of pressure increase. This phenomenon happened at different operating conditions but became more gradual with increasing the gas volume fraction. Large gas pockets were noticed at the pump suction during the surging conditions. Furthermore, recirculation bubble flows of different magnitudes were noticed at many locations between blades, in the inlet, and also at the outlet. The visualization experiments showed that the shape of most of the bubbles was not spherical but prolate spheroid. The size of the bubble was observed to be larger at a high gas volume fraction. This observation was attributed to the bubble coalescence inside the pump [50].

Also, Zhang et al. [51] conducted experiments of a similar nature in order to observe and explain the flow field present within a three-stage multiphase pump, particularly at the entrance section and in the sections containing the impeller. They analyzed the patterns of flow in the gas-liquid two stages using high-speed photographic equipment and ran the test pump under a variety of different settings to see how each affected the flow. The findings of the study revealed that the flow pattern at the entrance section was bubbly, indicating that the diameter of the bubbles grew larger as the gas volume percentage at the intake was increased, but that the size of the bubbles shrank as the rotating speed was increased. When the operation parameters were changed, it was found that the impeller had a variety of different flow patterns.

Later on, Verde et al. [52] conducted detailed research that was similar to the above one but with a focus on the impeller region. They developed an experimental rig that permitted the observation of the flow inside the impeller and used a high-speed camera to capture the flow pattern there. The findings substantiated that the flow style within the impeller significantly contributed to the deterioration of pump efficiency. Based on the water and air flow rates, different flow patterns were reported from the study. When the gas volume fraction is very low, small bubbles of different shapes, spherical or spheroid, suspended in the water phase are seen, and the flow pattern is bubbly. It was noticed in this case that the bubble size depended on the pump speed and was reversely proportional to the pump rotation speed. By increasing the gas flow, the flow pattern turned to agglomerated bubble flow, which is characterized by bubble interaction and coalescence and hence the formation of relatively larger bubble sizes in slow movements. A further increase in gas flow rate resulted in enhanced bubble coalescence and the formation of large and almost stationary bubbles. Only small bubbles could move downstream and form a turbulent recirculation region [53]. The flow pattern corresponding to these characteristics was referred to as a gas pocket flow pattern, and it resulted in the surging phenomenon. As the gas volume percent was increased, a segregated flow pattern developed in which elongated bubbles formed in isolation from one another [54]. Gas locking describes the situation in which the pump's performance drops too low and the pump head approaches zero.

Again, in another research project with similar objectives, In their study, Cubas et al. [55] did an experiment to look at the flow patterns inside a two-stage centrifugal pump and how well the pump managed a mixture of gas and liquid. The experiments started with using single-phase flow and obtaining the pump head curve to be compared with the one provided by the manufactured datasheet additionally, it can serve as a point of reference for investigations involving two-phase flow. The visualization experiments were carried out using a high-speed camera to see the gas-liquid patterns inside the centrifugal pump. The pump's performance was assessed based on the flow patterns observed under various operating situations. The results showed that four different flow patterns "bubble flow, agglomerated bubble flow, gas pocket flow, and annular flow" could be separated inside the impeller. These patterns changed depending on how fast the pump rotated and how much gas was in the fluid. These flow patterns had diverse impacts on the pump head and pump performance. When switching from bubble flow to an agglomerated bubble flow pattern, the effect on performance was reported to be very limited. On the other hand, when moving to an annular flow pattern, the influence became very significant. The surging phenomenon was also observed in this study in the gas pocket pattern when the gas pocket exited in all impeller regions. The researchers concluded that improving the pump's performance depended on controlling the pump speed, bubble size, and flow pattern. For example, increasing the pump speed could lead to minimizing the bubble sizes and, hence, permitting more gas flow without considerably affecting the pump's performance [56].

2.3 ANALYTICAL AND NUMERICAL WORK

Two-phase flow through centrifugal pumps is a crucial fluid dynamics topic with ramifications for many industries and applications. Centrifugal pumps, known for their efficiency and reliability, are used in oil and gas, industrial, and other industries to flow fluids smoothly. However, dynamics in two-phase flows—liquid-gas mixtures—are more complex and require further study.

This research explores two-phase flow in centrifugal pumps, its significance, and its many methods. Understand the complicated relationship between liquid and gas phases in the pump's operational setting, which affects efficiency, stability, and performance. The study uses numerical simulations, experimental studies, visualization tools, and analytical insights to provide a complete grasp of the issue.

As mentioned earlier, because of the complexity of the multi-phase flow pumping problems, the analytical and numerical studies in this field are challenging. Patil et al. [57] carried out a numerical study to assess the hydraulic performance of an electric submersible pump with fluids of different viscosities at high-speed using the CFD technique. The objective of the study was to observe the fluid pattern variations and evaluate the pump's performance as a function of rotational speed. The results showed that increasing the pump speed led to an enhancement in its performance due to the decrease in overall losses through the pump. This study also aimed at defining a numerical model for two-phase flow and understanding the parameters affecting the performance of the pump under two-phase flow conditions.

Minemura et al. [22] analytically analyzed the changes in the performance of centrifugal pumps that handle two-phase (air-water) flow at different air volume fractions using a separated flow model. The researchers also measured the size of air bubbles throughout the centrifugal pump. The results included a derivation of expressions that were used in two-phase flow pumping to determine the pump head, hydraulic losses, pressure-loss ratio, head-loss ratio, and bubble sizes. Regarding the bubble size, the main focus of the article, the results displayed a great uniformity in bubble sizes with relatively small diameters at the impeller inlet. However, further down, the uniformity was lost, and the bubble sizes started to grow as a result of bubble coalescence.

Zhu and Zhang [58],[59] numerically modelled various bubble sizes with different gas volume fractions inside the impeller of a submersible pump. They used a 3D CFD program, ANSYS CFX 15, to model and simulate the flow inside a three-stage centrifugal pump under different conditions. The governing equations, with the aid of the Eulerian-Eulerian approach and the k- ε turbulence model, were solved on a properly meshed computational domain. The results were validated by comparing them with pump performance curves from the catalog and also with the relevant experimental data. The results showed that the bubble size played a vital role in the centrifugal pump's performance and the ability to estimate its magnitude. For cases of low gas volume fractions, the numerical simulation using constant bubble sizes matched well with the reference experimental data. In contrast, for high gas volume fractions, there was a clear difference between the numerical and experimental measurements. Fortunately, the model with a larger stable bubble size could match the experimental data and correctly predict the increasing pressure through the pump stages.

A numerical simulation of an electrical submersible pump was carried out by Caridad et al. [60] with a particular emphasis on the impeller component of the pump. A combination of air and water was used as the operating fluid. During the course of the experiment, the head of the impeller, the phase distribution within the impeller, and the variations in outlet flow angle caused by changes in the flow rate of the liquid were all taken into consideration. In addition to this, the study included an investigation into how the observed parameters were affected by the gas volume fraction and bubble diameters. The CFD model in the study was a centrifugal impeller with seven blades, with a computational domain that included some distances before and after the blades to capture the flow physics upstream and downstream. The Navier-Stokes equations, together with a non-homogeneous two-phase flow model and a k- ε model for turbulence, were solved. The simulation included different cases, including gas volume fractions of 0 (single phase flow), 10, and 15%, and bubble diameters of 0.1, 0.3, and 0.5 mm. The results showed that with increasing the gas volume fraction, the gas phase accumulated, and gas pockets formed inside the impeller. This caused increased losses and reduced the pump head significantly. The pump head was further negatively affected by increasing the bubble size. The numerical results were compared with relevant experimental measurements and showed that CFD is a very powerful tool for analyzing two-phase flows in turbomachinery.

Zhang et al. [61] carried out a numerical simulation aiming at investigating the two-phase flow inside the impeller, considering the variation of the bubble size due to break-up or coalescence processes. They modified the typically used Euler model by introducing the secondary development technology of ANSYS CFX 16 and also by applying the non-uniform bubble model. The flow characteristics and phase interactions were analyzed at different inlet gas concentrations. Increasing the gas volume fraction resulted in an enhanced bubble breakup or coalescence process, and hence the gas could accumulate and the transformation to a gas pocket or segregated flow could occur. Introducing the developed model could reduce the relative error between the numerical and experiment data to an acceptable limit of less than 10%. It was illustrated that the need to apply the suggested modifications became more noticeable as the number of bubbles increased.

Pineda et al. [62] employed the VOF model to conduct a computational fluid dynamics (CFD) simulation investigation of the liquid-gas flow within a centrifugal pump. The investigation examined both the gas volume percent at the input and the pump head. The CFD simulation was conducted for the three-dimensional geometry of a one-stage pump using STAR-CCM+ commercial software. The findings indicated that augmenting the gas flow rate and reducing the pressure resulted in an expansion of the void fraction while concurrently leading to a drop in the pump head. Moreover, the findings revealed that augmenting the pump's rotational speed did not alter the average void fraction but led to a greater escalation in the fluctuation values. The difference between the numerical data and the experimental measurement exceeded 25%. The authors attributed this high error to the surging phenomenon noticed at high pump speeds.

Shi et al. [63] looked into whether gas-liquid multiphase pumping might have better transport performance. For this, they employed computational fluid dynamics (CFD) tools and an orthogonal test design approach. Different concentrations of gas and flow rates were used to calculate the head and efficiency index. Different pump parameters, such as diffuser blade numbers and angles as well as impeller dimensions, were included in the investigation. An ANSYS CFX program was used to do the CFD simulation; a two-phase Eulerian-Eulerian model and a k-*w* (SST) turbulence model was employed. To ensure a stable flow, the computational domain included, Besides the impeller and diffuser, pumps also require a specific amount of piping both before and after the device. The findings indicated that multiple factors influenced the head of the pump and its effectiveness, with the blade shroud angle being the most significant among them. The optimized design could improve the flow characteristics in general and, specifically, at an operating condition that corresponds to a gas volume percentage at the input of 15%, raise the head by approximately 3 meters and increase the efficiency by approximately 6%.The study also highlighted the CFD package's capacity to analyse two-phase flows and offered a crucial theoretical foundation for the enhancement and development of multiphase pumps. Finally, Hasan et al. [64] centrifugal pump flow pattern under two-phase flow situations as a function of pump rotation speed was considered. They carried out a numerical study using ANSYS Fluent software on the flow of gas and liquid mixtures at a constant flow rate, with a constant gas volume fraction, but with varying the pump rotational speed between 500 and 2500 rpm. The Navier-Stokes equations are solved, the Eulerian-Eulerian model is utilized for modeling the two-phase flow, and the k- ε model is employed for turbulence modeling. The results showed that when the rotational speed was low, a large gas pocket was observed at the inlet of the impeller. This gas pocket was noticed to be collapsed, and the flow pattern was turned into a bubby flow by increasing the pump speed.

2.4 FINAL REMARKS

This chapter conducts a thorough investigation of previous experimental and numerical research on the flow of two phases within centrifugal pumps. The primary objective of this review has been to examine alternative two-phase flow patterns at varying gas volume fractions and comprehend their impact on pump head and overall achievement. Although many studies have examined the behavior of centrifugal pumps in situations where two different phases are present, there is still a clear requirement for additional research in order to have a more profound comprehension of the intricacies included. The inherent complexity of the pump's geometry poses challenges in terms of visualizing and characterizing the intricate flow structures within centrifugal pumps through experimental means. In response, CFD simulation software emerges as a potent tool for depicting these flow patterns, offering a platform to convey detailed insights into the interplay between the phases and their subsequent impact on pump performance. However, due to the inherent complexities entailed in simulating two-phase flows, only a limited number of scholarly articles delve into this subject matter, thus underscoring the necessity for additional research endeavours to achieve a comprehensive understanding.

The main purpose of this endeavor is to utilize the ANSYS Fluent software to model the dynamics of two-phase flows in centrifugal pumps. The study aims to scrutinize a multitude of parameters that exert influence on pump performance, encompassing a broader spectrum of gas volume fractions, rotational speeds, and bubble sizes. The intention behind this investigation is to discern their collective effects on flow dynamics, pump pressure, and overall efficiency.

The anticipated outcome of this research is a plethora of results derived from the simulations. These findings are poised to serve as a foundation upon which suggestions for augmenting pump efficiency can be formulated and explored. By meticulously dissecting and interpreting the data garnered from the simulations, the study endeavours to illuminate avenues for optimizing pump performance, thereby contributing to the wider body of knowledge within the realm of centrifugal pump engineering.

In conclusion, this chapter lays the groundwork for a meticulous exploration of two-phase flow phenomena within centrifugal pumps. It emphasizes the role of experimental and numerical studies, acknowledges existing knowledge gaps, and underscores the importance of delving deeper into this complex field. The goal of the study is to find ways to improve the efficiency and performance of centrifugal pumps in real-world applications. This will be done by using advanced simulation tools and doing a deep analysis of how different factors affect the pumps.

3. MATHEMATICAL MODELLING

3.1 COMPUTATIONAL FLUID DYNAMICS

In many engineering systems, it is essential to acquire detailed information about flow behavior within the system. The experimental procedures can produce useful measurements, but unfortunately, these procedures consume a lot of time and money. Furthermore, it is not always possible to obtain detailed measurements experimentally for different practical and technical problems. The equations that govern fluid flow problems are non-linear, coupled partial differential equations. In most cases, except for a few cases of simple laminar flow problems, it is very difficult, if not impossible, to obtain an analytical solution for such equations. The numerical solution utilizing computers is an alternate technique for solving the governing mathematical equations and generating the necessary data. CFD includes the processes of obtaining numerical approximations to the solution of the equations that govern fluid flow and of heat transfer problems [65]

The CFD techniques have been significantly developed and widely used during the second half of the previous century[66]. The tremendous progress in computer science in recent years has made it possible to numerically solve even very complex flow problems using CFD techniques and obtain detailed knowledge about flow field parameters, including measurements that cannot be obtained experimentally. Nevertheless, the word "approximation" mentioned in defining CFD truly implies that the solutions obtained using CFD techniques contain some kind of error. This is particularly true when dealing with systems under turbulent flow conditions, where predicting flow behavior is difficult due to turbulence characteristics. Understanding the error sources and how to reduce them to the lowest possible level is crucial to the successful use of CFD techniques. In most cases, it is important to validate the numerical codes in order to assure that they produce accurate and reliable data [67],[68].

For a long time, commercial and in-house-developed CFD codes were widely used in various engineering systems and applications, including turbomachinery, aerodynamics, power plants, and several other different disciplines. These CFD packages have produced detailed, accurate data for single-phase flows, including pressure, velocity, temperature, and other flow parameters [69]. For two-phase flows, the great development in computer processors during the recent years, as well as the development in CFD codes and the availability of introducing various two-phase flow models, have significantly contributed to the CFD packages being essential in such investigations [36],[70].

The current study used the ANSYS Fluent commercial CFD program, which consists of three primary stages: pre-processing, solution, and post-processing.

In the first stage, After the computational domain has been created, it is subsequently partitioned into several smaller subdomains using a grid or a mesh. The mesh can be structured or unstructured, with elements of different shapes and sizes. The fluid properties are defined and stored in the mech cells, and finally, appropriate conditions at the domain boundaries are selected.

The second stage, solving, includes two main steps:

a. approximating the partial differential equations that govern the flow physics by means of a series of algebraic equations linking the parameters stored in the mech cells; this step is called discretization. Step
b. It encompasses the resolution of the discretized equations. Both the discretization itself and the solution of the resulting discretized equations can be accomplished in a variety of ways. The most important method for discretization is the Finite Volume Method (FVM), which is standard in heat and fluid flow problems and is utilized in most, if not all, commercial CFD software. This discretization method has many advantages, among them that it can accommodate any complex geometry and is conservative by nature. The solution methods are usually iterative, and the choice of a particular solution method depends on the form of the discretized equations [68],[71]. The third stage of the CFD procedure includes analyzing and presenting the large set of data files generated by the problem solver. The results presentation can take the form of vector and contour plots, x-y plots, or other kinds of plots showing the profiles of involved variables.

3.2 GOVERNING EQUATIONS

3.2.1 Single-Phase Flow

The single-phase flow is analyzed using ANSYS Fluent software by solving Reynolds-Averaged Navier Stocks (RANS) equations. These equations are derived by applying the main conservative principles of conservative mass and conservative momentum to a selected flow model and then taking the time average. If heat transfer is involved in the problem, the energy equation, which is a mathematical representation of the energy conservation law, must also be included. The RANS equations for incompressible three-dimensional flows are given by the following tensor forms [72]:

$$\frac{\partial \rho}{\partial t} + \frac{\partial(\rho \bar{U}_i)}{\partial x_i} = 0 \tag{3.1}$$

$$\rho \frac{\partial \bar{U}_i}{\partial t} + \rho \bar{U}_j \frac{\partial \bar{U}_i}{\partial x_j} = -\frac{\partial \bar{P}}{\partial x_i} + \frac{\partial}{\partial x_j}\left[\mu\left(\frac{\partial \bar{U}_i}{\partial x_j} + \frac{\partial \bar{U}_j}{\partial x_i}\right) - \rho \overline{u_i' u_j'}\right] \tag{3.2}$$

All symbols in equations (3.1) and (3.2) have their usual meanings. The i subscript in equation (3.2) represents the three coordinates in the Cartesian system, i.e., equation (3.1) is written once for each direction.

The equations (3.1) and (3.2) are of the same form as the well-known Navier-Stocks (NS) equations, apart from the appearance of fluctuating component correlations $-\rho\overline{u_i' u_j'}$. These new unknown terms are called turbulent or Reynolds stresses, and they need to be evaluated using extra equations in order to close the RANS equations. This is what is called turbulence modeling." The reliability of the solution is heavily dependent on the turbulence model that is chosen. The most widely used turbulence models EVMs . In these models, The Boussinesq hypothesis establishes a connection between Reynolds stresses and average velocity gradients, such as [73]:

$$\rho\overline{u_i' u_j'} = -\mu_t\left(\frac{\partial \bar{U}_i}{\partial x_j} + \frac{\partial \bar{U}_j}{\partial x_i}\right) + \frac{2}{3}\rho k \delta_{ij} \tag{3.3}$$

Where k is the turbulent kinetic energy, δ_{ij} is the Kronecker delta (1 if i = j , 0 otherwise), and μ_t is the turbulent or eddy viscosity.

Numerous models exist for simulating turbulent or eddy viscosity; these models are categorized into zero-, one-, and two-equation models categorized by the large number of transport equations they utilize. The last category is more popular and can produce more accurate results for different flow conditions compared to the other categories. The k - ε model is a popular type of two-equation turbulent model that uses the solution of one equation to get the kinetic energy k and the solution of the other equation to determine the turbulent dissipation rate. [74] . This model is employed in the current investigation, as determined by the literature evaluation outlined in Chapter 2. The equation provided in this model defines the turbulent viscosity.

$$\mu_t = \rho C_\mu k^2/\varepsilon \tag{3.4}$$

The constant C_μ has a value of 0.09. The transport equations for k and ε are in the following form:

$$\frac{\partial(\rho k)}{\partial t} + \frac{\partial(\rho k \bar{U}_j)}{\partial x_j} = P_k - \rho\varepsilon + \frac{\partial}{\partial x_j}\left[\left(\mu + \frac{\mu_t}{\sigma_k}\right)\frac{\partial k}{\partial x_j}\right] \tag{3.5}$$

$$\frac{\partial(\rho\omega)}{\partial t} + \frac{\partial(\rho\omega\bar{U}_j)}{\partial x_j} = C_{\varepsilon 1}\frac{\varepsilon}{k}P_k - C_{\varepsilon 2}\rho\frac{\varepsilon^2}{k} + \frac{\partial}{\partial x_j}\left[\left(\mu + \frac{\mu_t}{\sigma_\omega}\right)\frac{\partial\omega}{\partial x_j}\right] \tag{3.6}$$

where $P_k = -\overline{u_i' u_j'}\,\partial U_i/\partial x_j$ represents the turbulence generation rate, and the model constants are as follows: $C_{\varepsilon 1} = 1.44$, $C_{\varepsilon 2} = 1.92$, $\sigma_k = 1$, and $\sigma_\varepsilon = 1.3$.

$\sigma_\varepsilon = 1.3$, $\sigma_k = 1, C_{\varepsilon 1} = 1.44$,and $C_{\varepsilon 2} = 1.92$, are the model constants.

3.2.2 Two-Phase Flow

The Euler-Lagrange method and the Euler-Euler method are the two most commonly used ways to model two-phase flows. According to the Euler-Lagrange method, liquid is treated as a continuous phase, whereas gas is treated as a dispersed one. It is possible for the second dispersed stage and the primary liquid phase to trade mass, motion, and energy. Navier-Stocks (NS) equations are used to figure out the liquid phase, and the gas bubble paths are worked out one at a time at set points in the liquid phase calculation. This modeling method is well-suited for situations involving two-phase flow where the gas phase occupies a very small volume fraction. In the Euler-Euler approach, both phases are treated as continuous entities. The volume fraction for each phase is considered a continuous function across space and time, ensuring that the sum of the two-phase fractions remains constant at one throughout all spatial and temporal points. The continuity and momentum equations are individually solved for each phase, and these equations are connected through constitutive relations. The present work utilizes ANSYS FLUENT, a software that offers three distinct Euler-Euler multiphase models: the Eulerian model, the mixing model, and the VOF model [71]. The Eulerian model is used in this study, and hence it will be discussed in more detail in the following section.

3.2.2.1 Eulerian model

This model can be used to model two or more separate but interacting phases. In this study, two phases: liquid water (the primary phase) and air of fixed bubble sizes (the secondary phase) are used in the simulation. In this model, the pressure field is common for the two phases, while the velocity field and volume fractions are solved individually [71].

The continuity equation for phase q (liquid or gas) can be expressed as

$$\frac{\partial(\alpha_q\rho_q)}{\partial t} + \nabla.\left(\alpha_q\rho_q\vec{V}_q\right) = \sum_{p=1}^{n}\left(\dot{m}_{pg} - \dot{m}_{qp}\right) \tag{3.7}$$

where α_q represents the volume fraction of phase q, ρ_q is the density of phase q, $\vec{V}_q$ is the velocity vector of phase q, $\dot{m}_{pg}$ and $\dot{m}_{qp}$ represents the mass transfer rate from p^{th} phase to q^{th} phase and vice versa, respectively, and n is the number of phases (n = 2 for the present study). It is important to confirm that the sum of the phase volume fractions must be equal to unity this is :

$$\sum_{q=1}^{n}\alpha_q = 1 \tag{3.8}$$

Moreover, the momentum conservation results in an equation for phase (liquid or gas) of the form:

$$\frac{\partial}{\partial t}\left(\alpha_q\rho_q\vec{V}_q\right) + \nabla.\left(\alpha_q\rho_q\vec{V}_q\vec{V}_q\right) = \alpha_q\nabla\mathrm{p} + \nabla.\bar{\bar{\tau}}_q + \alpha_q\rho_q\vec{g} + \sum_{p=1}^{n}\left(\vec{R}_{pq} + \dot{m}_{pg}\vec{V}_{pq} - \dot{m}_{qp}\vec{V}_{qp}\right) + \left(\vec{F}_q + \vec{F}_{lift,q} + \vec{F}_{wl,q} + \vec{F}_{vm,q} + \vec{F}_{td,q}\right) \tag{3.9}$$

where $\bar{\bar{\tau}}_q$ represents the q^{th}phase stress-strain tensor and is defined by the expression

$$\bar{\bar{\tau}}_q = \alpha_q\mu_q\left(\nabla\vec{V}_q + \nabla\vec{V}_q^T\right) + \alpha_q\left(\lambda_q - \frac{2}{3}\mu_q\right)\nabla.\vec{V}_q\bar{I} \tag{3.10}$$

In equation (3.10) μ_q and λ_q represent the q^{th}phase shear and bulk viscosity.

The force $\vec{R}_{pq}$ represents the interaction between phases; $\vec{F}_q$ represents an external force acting on the system; $\vec{F}_{lift,q}$ represents the force of lift; $\vec{F}_{wl,q}$ represents the force of wall lubrication; $\vec{F}_{vm,q}$ represents the force of virtual mass; and $\vec{F}_{td,q}$represents the force of turbulent dispersion , and $\vec{V}_{pq}$, $\vec{V}_{pq}$ are the interphase velocities ($\vec{V}_{pq} = \vec{V}_p$ if $\dot{m}_{pg} > 0$ & $\vec{V}_{pq} = \vec{V}_q$ if $\dot{m}_{pg} < 0$ & $\vec{V}_{qp} = \vec{V}_q$ if $\dot{m}_{qp} > 0$ & $\vec{V}_{qp} = \vec{V}_p$ if $\dot{m}_{qp} < 0$). Other symbols in equations (3.9) and (3.10) have their usual meanings.

3.2.2.2 Closure relationships

The interaction between the two phases needs to be modelled in order to close the momentum equation and make it solvable. The interphase force can be modelled using the equation:

$$\sum_{p=1}^{n} \vec{R}_{pq} = \sum_{p=1}^{n} K_{pq} \left(\vec{V}_p - \vec{V}_q\right) \tag{3.11}$$

where this relation is subject to that $\vec{R}_{pq} = -\vec{R}_{qp}$ and $\vec{R}_{qq} = 0$, and $K_{pq} = K_{qp}$ The equation reflects the exchange of momentum between two phases. described in the following equation for the case of liquid-gas flow:

$$K_{pq} = \frac{\alpha_q \alpha_p \rho_p f}{\tau_p} \tag{3.12}$$

The variable f represents the drag function, while τ_p represents the particle relaxation period. The equation determines the τ_p:

$$\tau_p = \frac{\rho_p d_p^2}{18\mu_q} \tag{3.13}$$

where d_p is the diameter of the bubbles of the p^{th} phase. The f definition always include a drag coefficient (C_D). There are different models to calculate f, including Schiller and Naumann model [75] and Clift et al. model [76]. According to Schiller and Naumann model, the drag function is given by:

$$f = \frac{C_D Re}{24} \tag{3.14}$$

where the drag coefficient

$$C_D = \begin{cases} 24(1 + 0.15Re^{0.687})/Re & Re \leq 1000 \\ 0.44 & Re > 1000 \end{cases} \tag{3.15}$$

and the Reynolds number

$$Re = \frac{\rho_q \left|\vec{V}_p - \vec{V}_q\right| d_p}{\mu_q} \tag{3.16}$$

The gravitational, buoyant, and centrifugal forces are all included in the definition of the exterior body force , $\vec{F}_q$, As a consequence of the velocity gradient present in the main phase flow field, dispersed particles are subject to the lift force, denoted by the symbol , $\vec{F}_{lift,q}$,. The lift force is only significant for large particles, and thus it can be neglected for very small particles. It can be calculated based on Drew and Lahey [77] from the following equation:

$$\vec{F}_{lift,q} = -C_l \rho_q \alpha_p \left(\vec{V}_q - \vec{V}_p\right) \times \left(\nabla \times \vec{V}_p\right) \tag{3.17}$$

where the lift force coefficient, C_l, can be modelled using different forms, including that proposed by Legendre and Magnaudet [78] as

$$C_l = \sqrt{\left(C_{l,lowRe}\right)^2 + \left(C_{l,highRe}\right)^2} \tag{3.18}$$

$$C_{l,lowRe} = \frac{6}{\pi^2} Re_w^{-0.5} \frac{2.55}{\left(1 + 0.2\frac{Re_p^2}{Re_w}\right)^{1.5}} \quad \& \quad C_{l,highRe} = \frac{1}{2}\frac{1 + 16Re_p^{-1}}{1 + 29Re_p^{-1}} \tag{3.19}$$

Here, the particle Reynolds number, denoted as Re_p is defined by equation (3.16), and the vorticity Reynolds number, denoted as Re_w is defined as

$$Re_w = \frac{\rho_q \left|\nabla \times \vec{V}_q\right| d_p^2}{\mu_q} \tag{3.20}$$

The wall lubricating force, denoted as $\vec{F}_{wl,q}$, has a pushing effect on the flow of bubbles, causing them to move away from the limits of the wall. The general shape of it is as follows:

$$C_{wl} = max\left(0, \frac{C_{w1}}{d_b} + \frac{C_{w2}}{y_w}\right) \tag{3.22}$$

The non-dimensional coefficients C_{w1} and C_{w2} have values of -0.01 and 0.05, respectively. The variable d_b represents the bubble diameter, whereas y_w represents the distance to the next wall.

The accelerating bubbles experience the virtual mass force, denoted as $\vec{F}_{vm,q}$, with respect to the primary phase. The significance arises only when the density of the bubbles is considerably lower than the density of the primary phase. In steady-state simulation, which is commonly used for rotating machinery, the virtual mass force is disregarded. The virtual mass force is mathematically described by the following equation:

$$\vec{F}_{vm,q} = C_{vm}\rho_q\alpha_p\left(\frac{d_q\vec{V}_q}{dt} - \frac{d_p\vec{V}_p}{dt}\right) \tag{3.23}$$

Where C_{vm} is the so-called "virtual mass coefficient," and the value 0.5 is commonly used.

The turbulent momentum shift between phases is caused by the turbulent dispersion force, $\vec{F}_{td,q}$, the equation used to model it is:

$$\vec{F}_{td,q} = -\vec{F}_{td,p} = K_{pq}\vec{V}_{dr} \tag{3.24}$$

where $\vec{V}_{dr}$ is the drift velocity, that take the diffusion of bubbles flow as a result of the transport by turbulent fluid flow into account.

3.2.2.3 Turbulence modelling

The widely adopted model in simulations, known as the standard $k-\varepsilon$ model, is extensively used in both single-phase and two-phase simulations. In the context of two-phase flow scenarios, modifications are introduced to the model to account for turbulence within each phase. The transport equations governing turbulent kinetic energy (k) and energy dissipation rate (ε) take on specific forms to address the complexities of two-phase flow [79]:

$$\frac{\partial}{\partial t}\left(\alpha_q \rho_q k_q\right) + \nabla.\left(\alpha_q \rho_q \vec{U}_q k_q\right) = \nabla.\left[\alpha_q\left(\mu_q + \frac{\mu_{tq}}{\sigma_q}\right)\nabla k_q\right] + \alpha_q G_{k,q} - \alpha_q \rho_q \varepsilon_q + \alpha_q \rho_q \Pi_{kq} \tag{3.25}$$

$$\frac{\partial}{\partial t}\left(\alpha_q \rho_q \varepsilon_q\right) + \nabla.\left(\alpha_q \rho_q \vec{U}_q \varepsilon_q\right) = \nabla.\left[\alpha_q\left(\mu_q + \frac{\mu_{tq}}{\sigma_q}\right)\nabla \varepsilon_q\right] + \alpha_q \frac{\varepsilon_q}{k_q}\left(C_{1\varepsilon} G_{k,q} - C_{2\varepsilon} \rho_q \varepsilon_q\right) + \alpha_q \rho_q \Pi_{\varepsilon q} \tag{3.26}$$

Where Π_{kq} and $\Pi_{\varepsilon q}$ are source terms; $G_{k,q}$ is the production of turbulent kinetic energy; all other symbols have their usual meaning in one-phase flow model. The turbulent viscosity μ_{tq} is written in the form:

$$\mu_{tq} = \rho_q C_\mu \frac{k_q^2}{\varepsilon_q} \tag{3.27}$$

3.3 PUMP PERFORMANCE CHARACTERISTICS

3.3.1 Pump Head

Under single-phase conditions, the pump head can be represented by the following expression:

$$H = \frac{p_d - p_s}{\rho g} + \frac{V_d^2 - V_s^2}{2g} + (Z_d - Z_s) \tag{3.28}$$

where d and s subscripts denote downstream and upstream (suction), respectively. Under two-phase flow conditions, however, equation 3.28 must be modified to account for the changes in the gas-liquid mixture. Assuming that the two phases have the same velocity, the head equation becomes:

$$H = \frac{p_d - p_s}{\rho_{mix} g} + \frac{V_d^2 - V_s^2}{2g} + (Z_d - Z_s) \tag{3.29}$$

Where ρ_{mix} is the density of the two-phase mixture. In order to define the gas void fraction (α), it must be introduced. The gas void fraction and the two-phase density are defined by the following relations:

$$\alpha = \frac{Q_g}{Q_g + Q_l} \tag{3.30}$$

$$\rho_{mix} = \alpha \rho_g + (1 - \alpha)\rho_l \tag{3.31}$$

where Q is the flow rate, and the subscripts g and l stand for gas and liquid phases respectively.

3.3.2 Pump Efficiency

The efficiency of the pump is defined as the ratio between the fluid energy and the electric motor's energy (shaft power). That is,

$$\eta = \frac{P_{fluid}}{P_{Motor}} \tag{3.32}$$

For single phase flows, the energy consumed by the fluid is given by the following expression:

$$P_{fluid} = \rho g Q H \tag{3.33}$$

For two-phase flow conditions, on the other hand, the fluid energy is the sum of energy consumed by the liquid and gas phases, i.e.

$$P_{fluid} = P_{liquid} + P_{gas} \tag{3.34}$$

The liquid and gas energies are given by the following equations:

$$P_{liquid} = \rho g Q_l H \tag{3.35}$$

$$P_{gas} = \int Q_g dp \tag{3.36}$$

The motor power can be measured using a variable frequency drive (VFD), and assuming an electrical efficiency of 98%, the power consumed by the motor is given by the equation

$$P_{motor} = 0.98 P_{VFD} \tag{3.37}$$

3.4 CASE STUDY AND METHODOLOGY

In this study, three-dimensional CFD analysis is conducted on a single-stage centrifugal pump under two-phase flow conditions using the ANSYS program. The analysis focus is mainly on the impeller section and includes finding the pump specifications and phase distribution as a function of flow rate, gas volume fraction, and bubble sizes. Moreover, the analysis includes a validation study against well-obtained reference data prior to the main numerical investigation for more confidence in the results.

The next sections present and explain in depth the primary steps of the numerical simulation performed with the ANSYS commercial program.

3.4.1 Geometry and Computational Domain

The CFD model in the current study is a centrifugal impeller of seven blades, identical to that which has been previously experimentally tested by Anez et al. [80], the work used for the validation of the present numerical results. Table 3.1 shows the detailed geometrical dimensions of the impeller model. Taking advantage of the flow axisymmetric, only 1/7 of the geometry is modelled, and hence a huge saving in computational resources is attained. Figure 3.1 shows the CAD model of the impeller used for the analysis. Nevertheless, the computational domain is extended at the inlet and outlet in order to smooth any inconsistency that may arise due to turbulence and also to capture the flow physics upstream and downstream of the impeller.

Table 3.1: The Simulated Impeller's Geometrical Dimensions.

Dimension	Value
Impeller diameter, D_2 (mm)	82.7
Shaft diameter, D_{sh} (mm)	17.8
Tip to hub diameter ratio, D_2/D_1	2.22
Inlet blade angle, β_1 (deg.)	25
Outlet blade angle, β_2 (deg.)	30
Area (cm^2)	25
Blade height ratio, b_1/b_2	1.1
Number of blades, Z	7

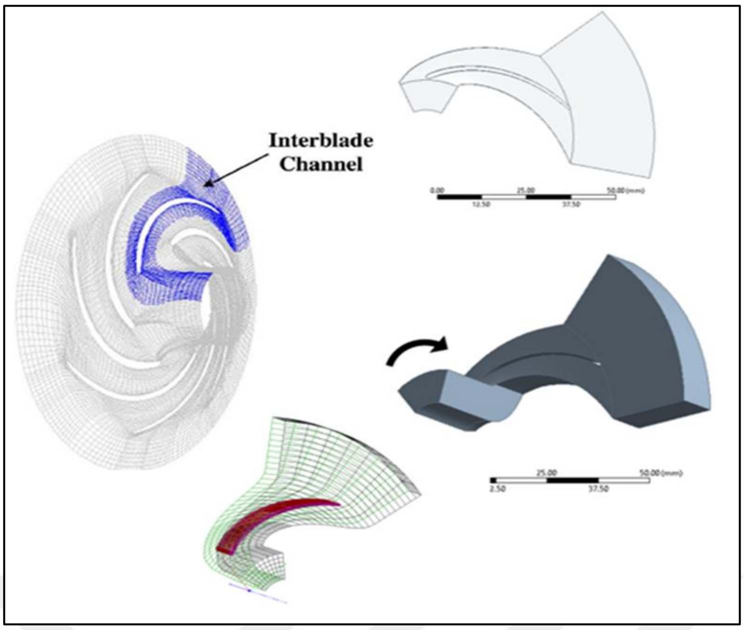

Figure 3.1: CAD Model of the Centrifugal Pump Flow Domain.

3.4.2 Mesh Generation

The computational domain is meshed using an unstructured, almost tetrahedral mesh with inflation layers. A mesh sensitivity analysis has been carried out to guarantee a mesh-independent solution. The total number of elements and nodes in the final examined mesh is 219919 and 66291, respectively. Figure 3.2 shows the meshed model of the computational domain.

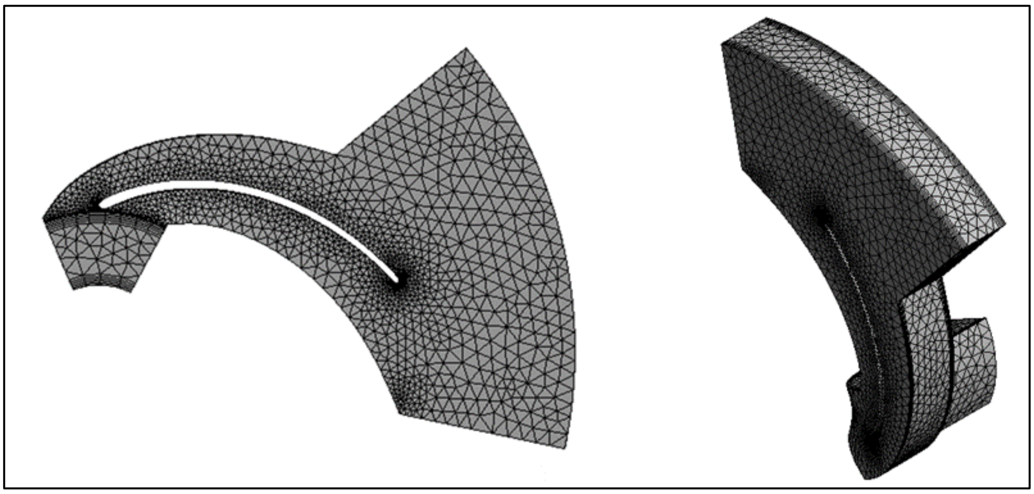

Figure 3.2: The Computational Domain Meshing.

3.4.3 Boundary Conditions

Figure 3.3 and Table 3.3 show the border conditions that were used on the impeller model. At the entrance, the total pressure stays the same, but at the domain's exit, a specific mass flow rate value is set. Furthermore, a periodic boundary is defined at the sides to account for the problem symmetry. Finally, no condition for slip velocity is imposed on any of the domain boundaries.

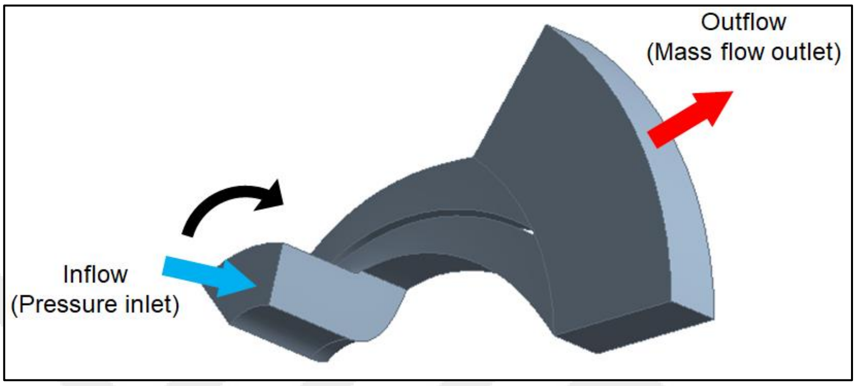

Figure 3.3: The Boundary Condition Imposed on the Inlet and Outlet of the Impeller.

Table 3.2: Boundary Conditions.

Boundary	Type
Inflow	Total inlet pressure (100000 Pa)
Outlet	Mass flow outlet
Shroud, Hub and blade	No slip wall
Side boundaries	Periodic boundary

3.4.4 Numerical Setting

The finite volume method, specifically the first-order backward difference scheme, is used to discretize the governing equations. The k-ε model is used to simulate turbulence in both one- and two-phase flows. The pressure and velocity fields are coupled and solved using a pressure-based coupling algorithm. For two-phase flow cases, the Eulerian approach is used to obtain the phases distribution and their impact on the pump characteristics. Different under-relaxation factors are applied for pressure and momentum terms in order to attain stable convergence. The convergence criteria are established with a minimum threshold of 10^{-3} for all quantities and equations during the solving process.

3.4.5 Results Validation

Prior to the main investigation, the numerical results of the current model were Initially, the validity of the results was established by comparing them with the empirical data provided by Anez et al. [80], who examined an impeller with the same specifications. The current data are also compared to the numerical results of Caridad et al. [60] for more confidence. Figure 3.4 represents the pump head data for the current simulation and the reference studies. The graph shows that the experimental data and the numerical data are pretty much the same. In fact, the latest results are a little better than the numerical data from Caridad et al. It should be noted, though, that the numerical simulation gives higher head values for all flow rates that were tried. It is thought that the biggest difference between the numerical results and the testing results is about 20%. This discrepancy has been attributed to the diffuser losses, which are not included in the numerical simulation [60]. Based on this analysis and discussion, it can be inferred that the existing numerical model and settings are capable of accurately predicting the flow within the impeller. Therefore, they can be utilized in future research instances.

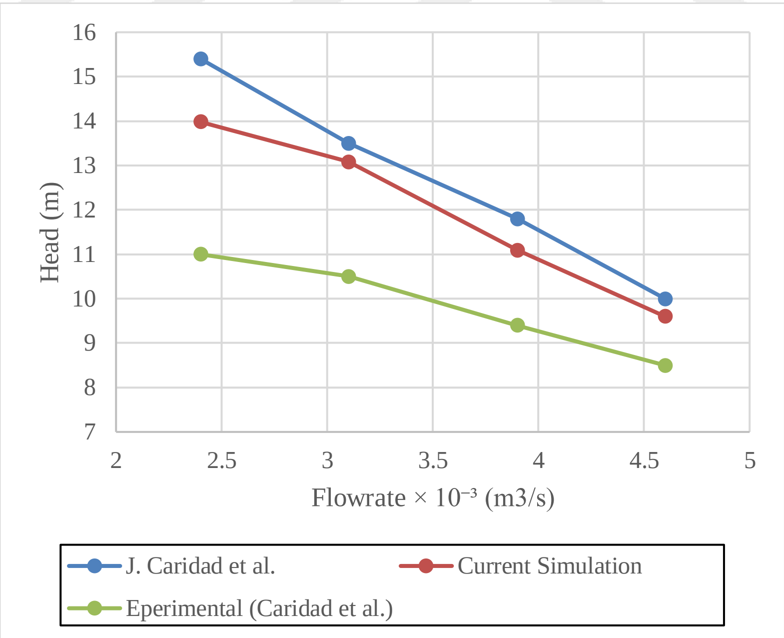

Figure 3.4: Comparison with Reference Experimental and Numerical Results**.**

4. RESULTS AND DISCUSSION

The current research includes a numerical investigation of two-phase flow inside a centrifugal impeller. The effect of flow rate, gas volume fraction (GVF), and bubble sizes on the head and efficiency of the pump and also on the phase distribution are determined in the simulation. The study also includes determining the variation of pump specifications as a function of flow rate under single-phase flow conditions. This is considered important to compare the pump performance under single- and two-phase flow conditions.

4.1 EFFECT OF FLOW RATE

4.1.1 Single-Phase Flow Conditions

Figure 4.1 illustrates the variations in pump head and efficiency at different water flow rates (2.4, 3.1, 3.9, and 4.6 kg/s). The total inlet pressure is 100000 Pa, and the rotational speed is 2500 rpm. The figure shows that increasing the flow rate is associated with decreasing both pump head and hydraulic efficiency. Increasing the volume flow rate leads to increased friction losses, reducing the total head that can be produced by the pump. Furthermore, the hydraulic efficiency also decreases with increasing the flow rate, within the tested range, particularly for relatively high flow rate values. The efficiency magnitude drops from about 56% to less than 52% by increasing the flow rate from 3.9 kg/s to 4.6 kg/s. The efficiency relation indicates that the efficiency value depends on the product of head and flow rate and on the power introduced to the pump. By increasing the flow rate beyond some value, the drop in head loss and the increase in required power into the system due to increasing friction losses overcome any efficiency gain those results from increasing the flow rate. Therefore, the efficiency continues to decrease with increasing flow rate, as figure 4.1 shows.

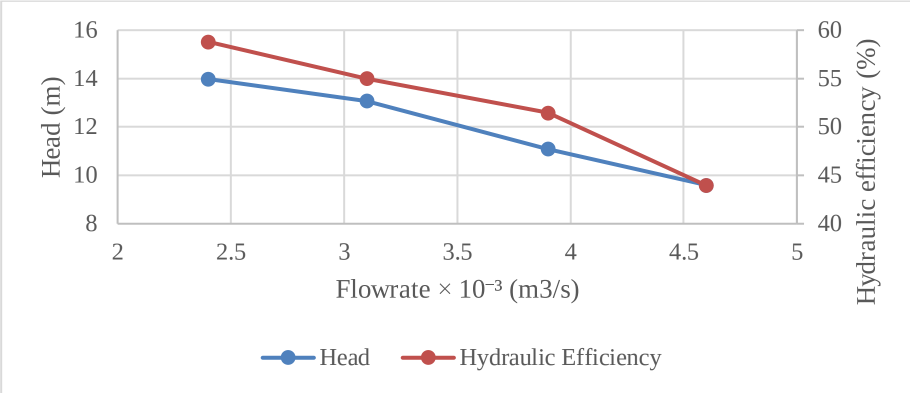

Figure 4.1: The Head and Effectiveness of the Centrifugal Pump in the Presence of Single-Phase Flow Circumstances.

4.2.2 Two-Phase Flow Conditions

The effect of flow rate on the impeller performance curves is also considered under two-phase flow conditions. Flow rate values identical to those tested for single-phase flow cases are included in the simulation. Not only flow rate values but also all other operation conditions are maintained similar to the previous case in order to compare impeller performance under different flow conditions. Figure 4.2 shows the head and hydraulic efficiency of the centrifugal impeller as a function of the flow rate under two-phase flow conditions, with GVF = 0.1 and a bubble dimeter = 0.1 mm. It can be seen that a similar behavior to that reported in the single-phase flow case is also observed in the two-phase flow condition. Both pump head and efficiency decrease with increasing flow rate. Nevertheless, under a two-phase flow condition, the reduction levels are more significant. Here, in addition to the increased system losses due to increasing the flow velocity (or flow rate), there is a negative effect of the gas.

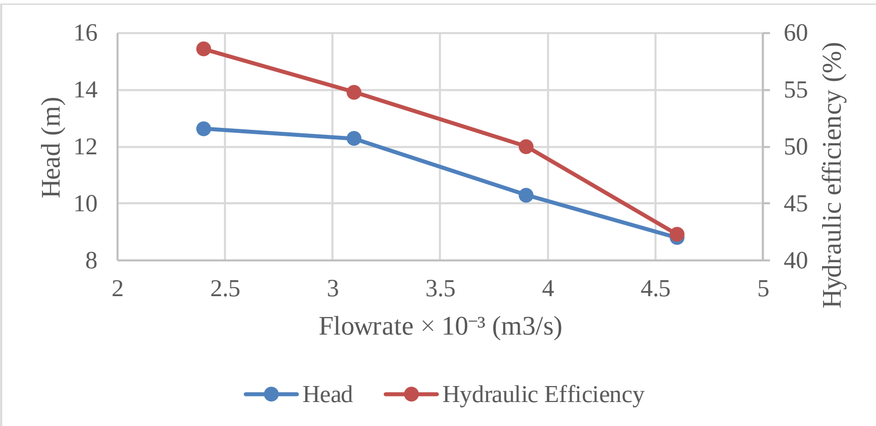

Figure 4.2: The Head and Efficiency of the Centrifugal Pump in the Presence of Single-Phase Flow Circumstances.

4.3 EFFECT OF GAS VOLUME FRACTION

The effect of increasing the GVF on the head, efficiency, and phase distribution is considered in the study. Four different GVF values—0.1, 0.15, 0.2, and 0.3—are included in the simulation. The mass flow rate is set at 2.4 kg/s, the bubble size is set at 0.1 mm, and the impeller rotation speed is set at 2500 rpm. Figure 4.3 represents the head and efficiency variations with the GVF. It can be noticed that for the tested flow rate, the pump head as well as the pump efficiency decrease almost linearly with increasing the volume fraction of the air. This agrees well with the observations in the relative literature [81] .Increasing the GVF from 0.1 to 0.3 causes the head to decrease by about 15% and hydraulic efficiency by up to 12%. This may be explained by the fact that the gas accumulation phenomena in the impeller and the degree of bubble coalescence may continue to increase by increasing the GVF, and as a result, the pump performance is seriously negatively affected.

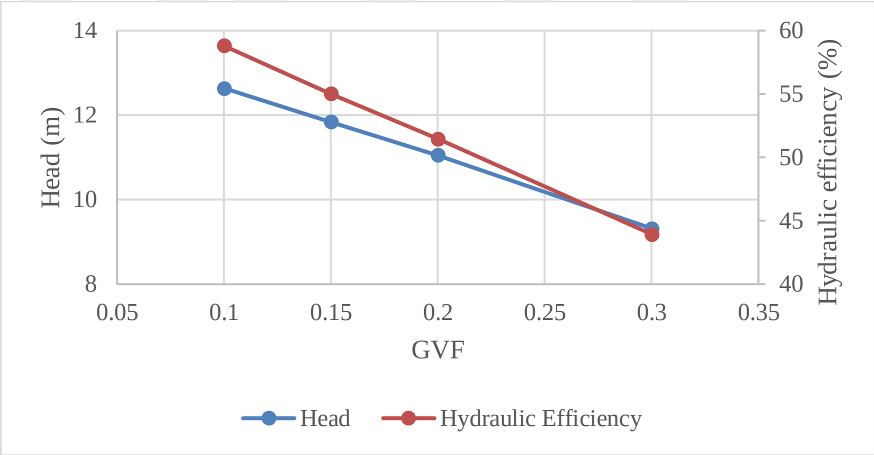

Figure 4.3: The Head and Efficiency Variations of the Centrifugal Pump with Increasing GVF, at Flow Rate 2.4 kg/s, Bubble Size 0.1 mm and Rotational Speed 2500 Rpm.

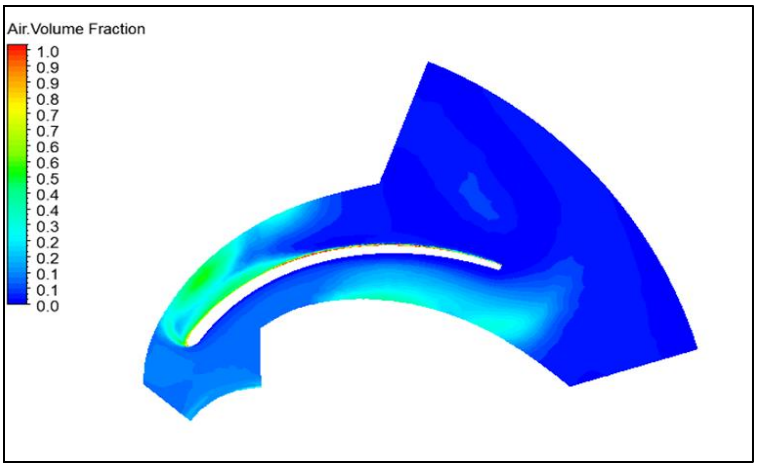

Figure 4.4: Cont. (a) Gas Phase Distribution with Increasing GVF.

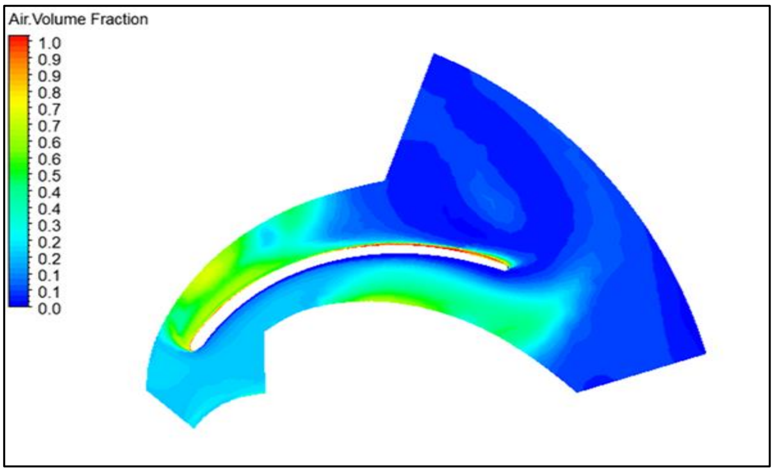

(b) Gas Phase Distribution with Increasing GVF.

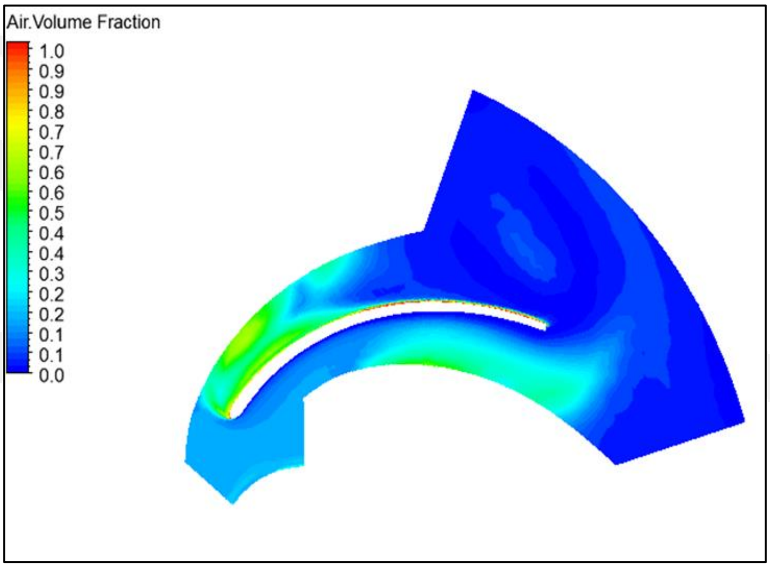

(c) Gas Phase Distribution with Increasing GVF.

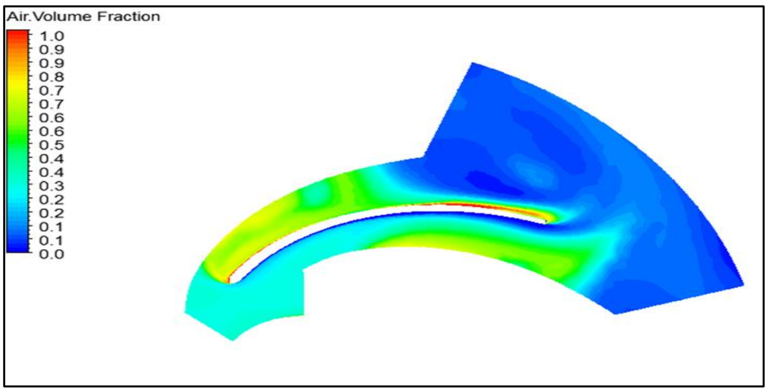

(d) Gas Phase Distribution with Increasing GVF.

Figure 4.4: Gas Phase Distribution with Increasing GVF at Flow Rate 2.4 kg/s, Bubble Sizes (a) 0.1 mm, (b) 0.15 mm, (c) 0.2 mm, (d) 0.30 mm, and Rotational Speed 2500 Rpm 'Figure Continued'.

A more detailed view of the gas phase distribution can be attained through the contours at different GVFs As depicted in Figure 4.4, the gas collection is evident as well as the bubble coalescence became more pronounced as the GVF increased. At low GVF = 0.1, the gas phase is primarily accumulated in the inlet area of the impeller, particularly on the blade upper surface. Because the density of the liquid is much greater than the gas density, the centrifugal force acts to accumulate the liquid phase at the edge, while the gas phase is accumulated near the hub. With increasing the GVF, the gas phase gradually extends through the impeller toward the exit and becomes more noticeable at different areas along the impeller. At high GVF = 0.3, the gas phase accumulation phenomenon is clearly observed, and gas pockets are formed. These findings have previously been confirmed by the results of some researchers, such as Verde et al.[58] and Zhang et al.[22] who have reported the transport to a gas pocket or segregated flow pattern at high GVF. They have claimed that this phenomenon can have a significant impact on pump performance and cause a considerable reduction in pump head and efficiency, as seen in Figure 4.3.

4.4 EFFECT OF BUBBLE SIZE

The current investigation also includes considering the effect of bubble diameter on the pump performance curves, the head, and efficiency variation. The phase distribution with changing bubble sizes is also visualized and discussed. In order to find the influence of bubble diameters on the two-phase flow inside centrifugal pumps, values of this variable are considered in the simulation, namely d = 0.1, 0.2, 0.3, and 0.5 mm for the cases corresponding to flow rates of 2.4 kg/s and 3.15 kg/s, the GVF at 0.1, and the impeller rotation speed at 2500 rpm. Figure 4.5 demonstrates the obtained results for the considered cases. It can be noted that for the two values of flow rates, both the pump head and efficiency decrease with increasing bubble diameter for small sizes. However, the degradation is much larger at high flow rates. By doubling the bubble diameter from 0.1 to 0.2, the impeller head is decreased by up to 10% for flow rate 3.15 kg/s,but is decreased by only about 3% for flow rate 2.4 kg/s. Almost similar behavior is observed for the hydraulic efficiency variations with increasing bubble size at small rates. Any further increase in bubble diameter has only a limited effect on the head and efficiency for the small flow rate, with a continuous slow decrease with increasing bubble sizes. For large flow rates, however, a reverse behavior is noticed, as both head and efficiency start to increase with increasing bubble sizes beyond 0.2 mm.

The usual behavior of decreasing the pump performance curves with increasing bubble size can be explained by means of the forces acting on the bubbles. At low flow rates, by increasing the bubble size, the force acting as a result of the adverse pressure magnifies more considerably than the drag force. Hence, as a result, the air pocket increases, and therefore the hydraulic losses increase, and the pump performance is negatively affected. For large bubble diameters, the effect is practically negligible or has an opposite direction, depending on the value of the flow rate. Larger liquid volumes lead to larger drag force values and, consequently, smaller gas pocket sizes.

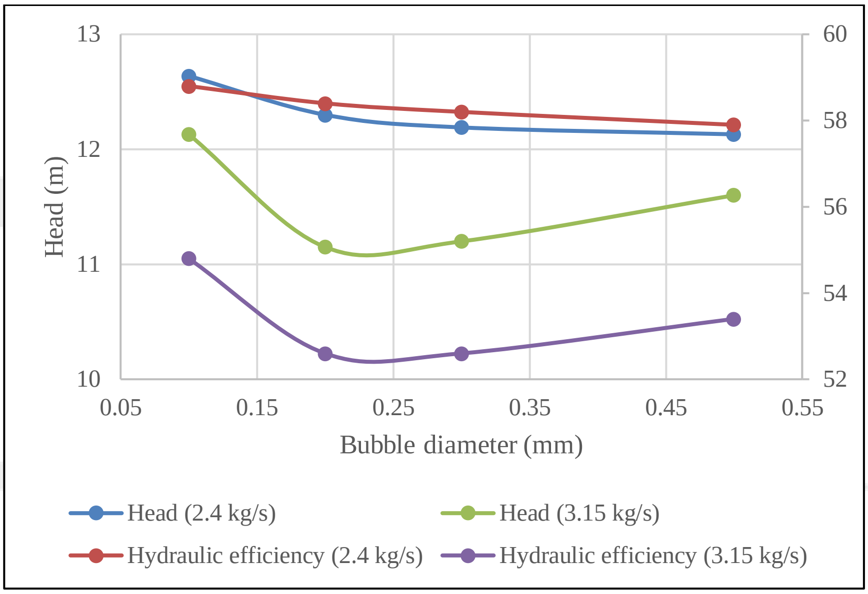

Figure 4.5: The Head and Efficiency Variations of the Centrifugal Pump with Increasing Bubble Diameter, at Flow Rate 2.4 kg/s & 3.15 kg/s, GVF = 0.1, and Rotational Speed 2500 Rpm.

Again, the phase distribution contours for the examined bubble sizes at GVF = 0.1 and flow rate 2.4 kg/s are displayed in figure 4.6. It can be seen from the figure that the areas of high gas volume fraction increase with increasing bubble diameters for identical GVF values. This is explained simply because larger bubbles occupy larger spaces, particularly when they accumulate together. Furthermore, the figure shows that air bubbles tend to aggregate at the impeller inlet, on the top pressure side of the blade, and then move further away when their volume enlarges. Gas pockets can be clearly seen at the inlet upper pressure side of the impeller blade and also far in the inter-blade channel for large bubble sizes, particularly at d = 0.5 mm. The head degradation reported in pumps that deliver two-phase flows has been explained by the impact of gas accumulation on hydraulic losses. The air aggregation on the pressure side of the blade is sustained by the influence of the drag force, and the force results from the pressure gradient acting on bubbles. Because of the velocity variation between the liquid and gas velocities, the drag force acts to drive the bubble far downward to the outlet. Since the pressure gradient is adverse, the force due to the pressure gradient acts to slow down the bubbles. These observations are in full agreement with many previous studies, including Caridad et al. [34] and Murakami & Minemura [20].

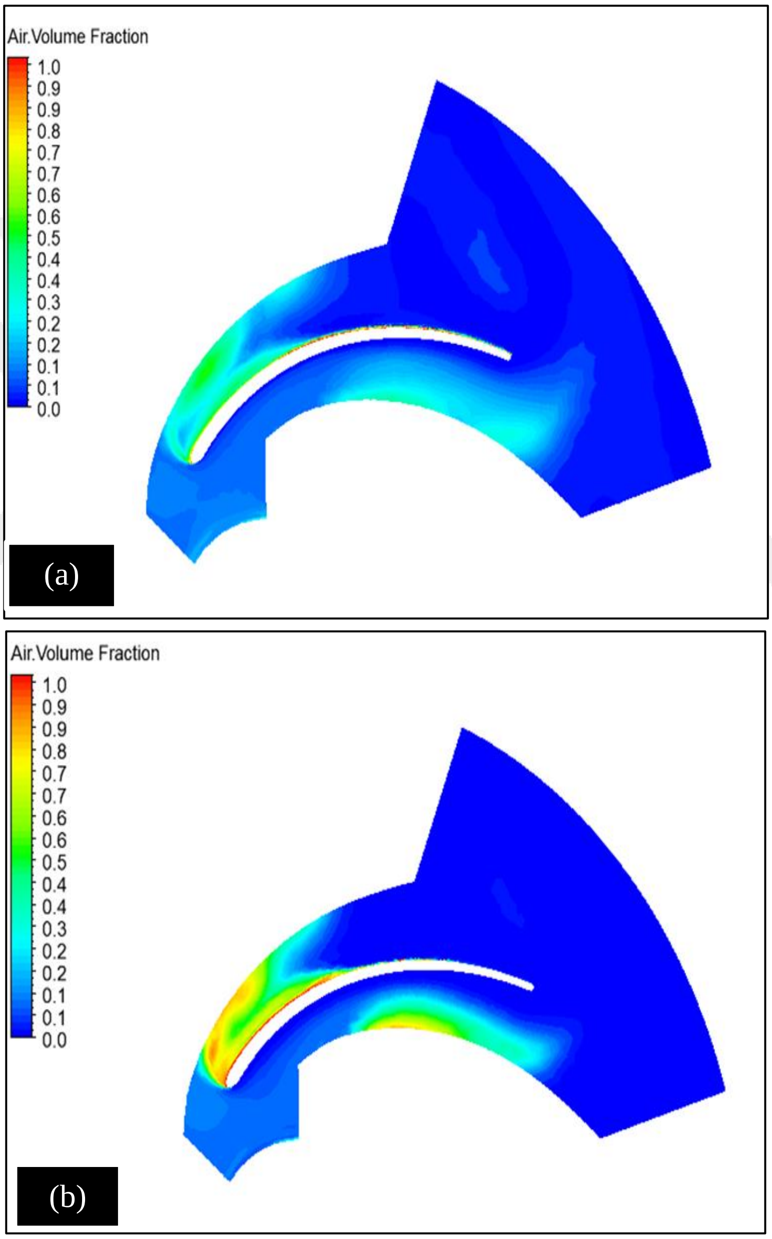

Figure 4.6: Gas Phase Distribution with Bubble Diameters (a) 0.1, (b) 0.2, (c) 0.3, (d) at Flow Rate 2.4 kg/s, GVF = 0.1, and a Rotational Speed of 2500 Rpm.

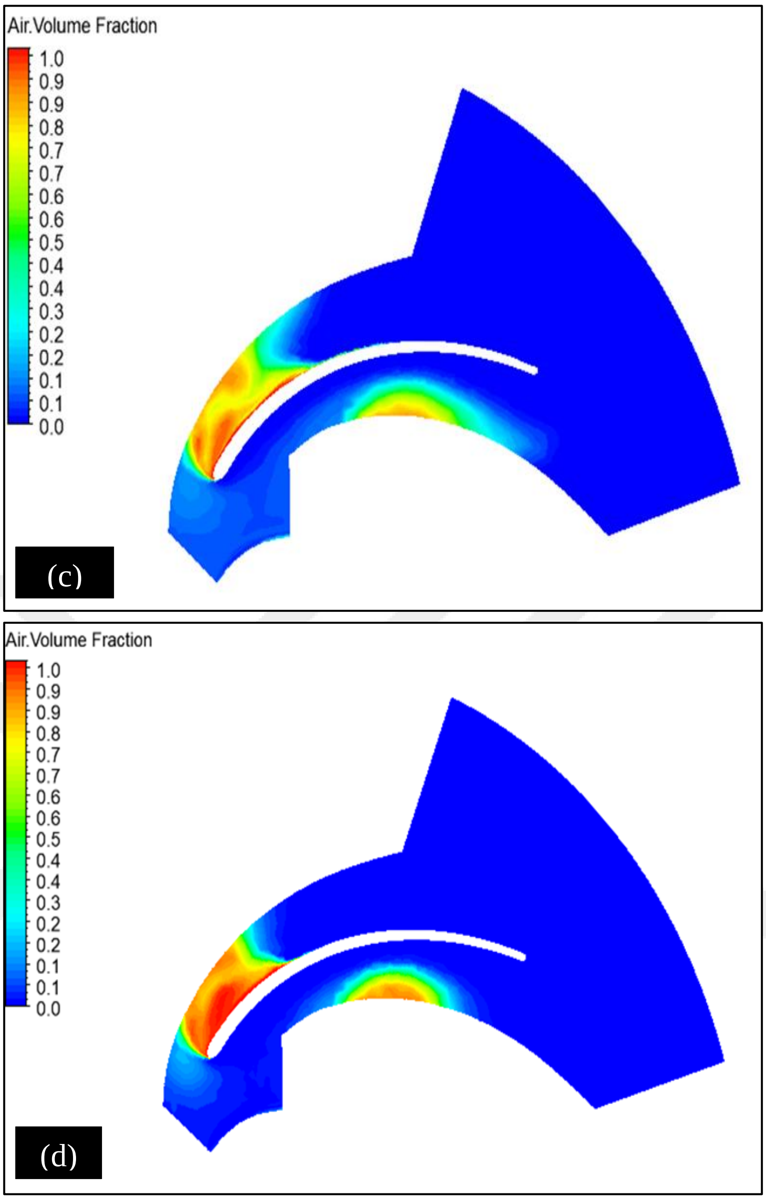

Figure 4.6: Gas Phase Distribution with Bubble Diameters (a) 0.1, (b) 0.2, (c) 0.3, (d) at Flow Rate 2.4 kg/s, GVF = 0.1, and a Rotational Speed of 2500 Rpm ‘Figure Continued’.

(d)

5. CONCLUSION AND RECOMMENDATIONS

5.1 CONCLUSIONS

Centrifugal pumps under two-phase flow conditions have many applications, including in the gas and oil industries. Two-phase pumping may be associated with many difficulties, resulting in a reduction in the overall performance of the pump compared to single-phase pumping. The gas accumulation on the impeller blade and the possibility of forming gas pockets can seriously affect the pump head and efficiency. Several factors can play important roles in the problem, including impeller geometry, gas volume fraction, bubble sizes, and rotational speed.

In the current study, a centrifugal impeller handling an air-water mixture of different specifications is simulated using ANSYS software. The effect of flow rate, air volume fraction, and bubble diameter on the pump performance curves, head, and efficiency are considered in the investigation. The operation under a single-phase flow condition is also considered for comparison purposes. The simulation also included the visualization of phase distributions at different GVF and bubble sizes. The inlet total pressure is set at 100000 Pa, and the rotational speed is set at 2500 rpm. The flow rate is varied in the range between 2.4 and 4.6 kg/s. Gas volume fractions at 0.1, 0.15, 0.2, and 0.3 and bubble diameters at 0.1, 0.2, 0.3, and 0.5 mm are considered in the simulation.

Based on the results of the present study, the following conclusions can be drawn:

a. For single- and two-phase flow conditions, increasing the flow rate results in decreasing both pump head and efficiency. However, the reduction is more pronounced in the two-phase flow case. The reduction is explained as a result of increasing system losses by increasing the flow rate.

b. Increasing the gas volume fraction causes a significant decrease in head and efficiency curves. Within the tested range, the values drop by more than 25% by increasing the GVF. This is attributed to the gas accumulation phenomena in the impeller that are clearly visualized through the gas distribution contours with increasing GVF.

c. The phase distribution at high GVF = 0.3 confirms the gas phase accumulation phenomenon and the formation of gas pockets on the high-pressure side of impeller blades.

d. Increasing the bubble size from 0.1mm to 0.2 mm causes a significant reduction in pump performance. However, the variation in the head and efficiency is either negligible or has a reverse effect, depending on the value of the flow rate. Large volume rates lead to a diminished gas pocket pattern as a result of acting forces.
e. The phase distribution contours for a small flow rate of 2.4 kg/s and different bubble diameters clearly show gas pockets at the inlet upper pressure side of the impeller blade and also far in the inter-blade channel, particularly for bubble diameters of 0.3 and 0.5 mm. This phenomenon is limited in the case of smaller bubble sizes.

5.2 RECOMMNDATIONS

The present study contributes toward enhancing the understanding of two-phase pumping and its related parameters. According to the outcome of the current research and the discussion and conclusions presented above, many research questions may be suggested for the forthcoming investigations in this field, including:

a. Studying the effect of changing the inlet pressure on the pump's performance.
b. Determining the effect of the rotational speed on pump parameters and also on the phase distribution.
c. Include the diffuser in addition to the impeller in the simulation in order to find the flow pattern variations after leaving the impeller.

REFERENCES

[1] G. Takacs, *Electrical submersible pumps manual: design, operations, and maintenance*. Gulf professional publishing, 2017.

[2] V. K. A. Shankar, S. Umashankar, S. Paramasivam, and N. Hanigovszki, “A comprehensive review on energy efficiency enhancement initiatives in centrifugal pumping system,” *Appl. Energy*, vol. 181, pp. 495–513, 2016.

[3] J. Wagner, *Membrane filtration handbook: Practical tips and hints*, vol. 129. Osmonics Cambrige, 2001.

[4] S. Ketelsen, D. Padovani, T. O. Andersen, M. K. Ebbesen, and L. Schmidt, “Classification and review of pump-controlled differential cylinder drives,” *Energies*, vol. 12, no. 7, p. 1293, 2019.

[5] A. Ali *et al.*, “Comparison of empirical models using experimental results of electrical submersible pump under two-phase flow: Numerical and empirical model validation,” *Phys. Scr.*, vol. 97, no. 6, p. 65209, 2022.

[6] T. Katke, “Analysis of Two-Phase Flow Through an Electric Submersible Pump Using Computational Fluid Dynamics.” 2020.

[7] Y. Fu *et al.*, “Numerical and experimental analysis of flow phenomena in a centrifugal pump operating under low flow rates,” *J. Fluids Eng.*, vol. 137, no. 1, p. 11102, 2015.

[8] M. E. Qazizada, V. Sviatskii, and P. Božek, “Analysis performance characteristics of centrifugal pump,” *MM Sci. J.*, vol. 10, 2016.

[9] J. R. Thome, “Engineering Data Book III, Wolverine Tube,” *Inc., Huntsville, Ala*, 2004.

[10] B. R. Patel, “Investigation into the Two-Phase Flow Behavior of Centrifugal Pumps,” in *Proc. Symp. on Polyphase Flow in Turbomachinery*, 1978, vol. 79.

[11] S. E. Downham, “Modelling the two-phase performance of a centrifugal pump,” 2000.

[12] X. Zhao, Y. Xiao, Z. Wang, Y. Luo, and L. Cao, "Unsteady flow and pressure pulsation characteristics analysis of rotating stall in centrifugal pumps under off-design conditions," *J. Fluids Eng.*, vol. 140, no. 2, p. 21105, 2018.

[13] C. T. Crowe, J. D. Schwarzkopf, M. Sommerfeld, and Y. Tsuji, *Multiphase flows with droplets and particles*. CRC press, 2011.

[14] R. M. Perissinotto *et al.*, "Flow visualization in centrifugal pumps: A review of methods and experimental studies," *J. Pet. Sci. Eng.*, vol. 203, p. 108582, 2021.

[15] R. Spence, "CFD Analyses of Centrifugal Pumps with Emphasis on Factors Affecting Internal Pressure Pulsations." Cranfield University, 2006.

[16] Q. Jiang, Y. Heng, X. Liu, W. Zhang, G. Bois, and Q. Si, "A review of design considerations of centrifugal pump capability for handling inlet gas-liquid two-phase flows," *Energies*, vol. 12, no. 6, p. 1078, 2019.

[17] J. F. Gülich, "Impact of three-dimensional phenomena on the design of rotodynamic pumps," *Proc. Inst. Mech. Eng. Part C J. Mech. Eng. Sci.*, vol. 213, no. 1, pp. 59–70, 1999.

[18] S. Chitale, P. Jadhav, S. Dhoble, and S. Deshmukh, "Parameters affecting efficiency of centrifugal pump-A review," *Int. J. Sci. Res. Sci. Technol.*, vol. 8, no. 6, pp. 49–58, 2021.

[19] L. Szalinski *et al.*, "Comparative study of gas–oil and gas–water two-phase flow in a vertical pipe," *Chem. Eng. Sci.*, vol. 65, no. 12, pp. 3836–3848, 2010.

[20] T. Y. Makogon, *Handbook of multiphase flow assurance*. Gulf Professional Publishing, 2019.

[21] L. Wang, H. Cheng, T. Yang, Y. Zhao, W. Yuan, and K. Ren, "Study of the operating characteristics of a pump-driven thermosyphon loop with gas–liquid separation," *Appl. Therm. Eng.*, vol. 234, p. 121265, 2023.

[22] J. Zhang, S. Cai, Y. Li, H. Zhu, and Y. Zhang, “Visualization study of gas–liquid two-phase flow patterns inside a three-stage rotodynamic multiphase pump,” *Exp. Therm. Fluid Sci.*, vol. 70, pp. 125–138, 2016.

[23] D. Kernan, “Pumps 101: Operation, Maintenance and Monitoring Basics,” *White Pap. Monit. Control Group. ITT*, 2009.

[24] J. Ancheyta, *Modeling of processes and reactors for upgrading of heavy petroleum*. CRC Press, 2013.

[25] I. Urbina-Salas *et al.*, “Application of convolutional neural networks for the classification of two-phase flow patterns,” in *2021 IEEE International Autumn Meeting on Power, Electronics and Computing (ROPEC)*, 2021, vol. 5, pp. 1–6.

[26] R. Wajman *et al.*, “Metrological evaluation of a 3D electrical capacitance tomography measurement system for two-phase flow fraction determination,” *Meas. Sci. Technol.*, vol. 24, no. 6, p. 65302, 2013.

[27] G. Besagni, F. Inzoli, and T. Ziegenhein, “Two-phase bubble columns: A comprehensive review,” *ChemEngineering*, vol. 2, no. 2, p. 13, 2018.

[28] E. Gharaibah, A. Read, and G. Scheuerer, “Overview of CFD multiphase flow simulation tools for subsea oil and gas system design, optimization and operation,” in *Offshore Technology Conference Brasil*, 2015, p. D011S003R004.

[29] D. S. N. T. F. Vignat, “Deviations throughout Its Life Cycle.”

[30] W. Zhao and G. Zhao, “Numerical investigation on the transient characteristics of sediment-laden two-phase flow in a centrifugal pump,” *J. Mech. Sci. Technol.*, vol. 32, pp. 167–176, 2018.

[31] G. Besagni and F. Inzoli, “The effect of liquid phase properties on bubble column fluid dynamics: Gas holdup, flow regime transition, bubble size distributions and shapes, interfacial areas and foaming phenomena,” *Chem. Eng. Sci.*, vol. 170, pp. 270–296, 2017.

[32] P. Girdhar, “Centrifugal Pumps.” New York, 2005.

[33] A. Serena, “A multiphase pump experimental analysis,” 2016.

[34] A. Patil, W. Yin, R. Agarwal, A. Delgado, and G. Morrison, “Extending classical friction loss modeling to predict the viscous performance of pumping devices,” *J. Fluids Eng.*, vol. 141, no. 10, p. 101202, 2019.

[35] W. D. Schmidl, *Three-dimensional experimental investigation of the two-phase flow structure in a bubbly pipe flow*. Texas A&M University, 1999.

[36] W. Zhang, Z. Yu, M. N. Zahid, and Y. Li, “Study of the gas distribution in a multiphase rotodynamic pump based on interphase force analysis,” *Energies*, vol. 11, no. 5, p. 1069, 2018.

[37] G. Takacs, *Sucker-rod pumping handbook: production engineering fundamentals and long-stroke rod pumping*. Gulf Professional Publishing, 2015.

[38] S. Levy, *Two-phase flow in complex systems*. John Wiley & Sons, 1999.

[39] R. Ramirez, E. Avila, L. Lopez, A. Bula, and J. D. Forero, “CFD characterization and optimization of the cavitation phenomenon in dredging centrifugal pumps,” *Alexandria Eng. J.*, vol. 59, no. 1, pp. 291–309, 2020.

[40] M. W. Shahzad, M. Burhan, L. Ang, and K. C. Ng, “Energy-water-environment nexus underpinning future desalination sustainability,” *Desalination*, vol. 413, pp. 52–64, 2017.

[41] H. M. Ramos *et al.*, “Concerning dynamic effects in pipe systems with two-phase flows: Pressure surges, cavitation, and ventilation,” *Water*, vol. 14, no. 15, p. 2376, 2022.

[42] J. Silva, P. Vaz, P. Martins, and L. Ferreira, “Reliability Estimation for Industrial Equipment Using EM Algorithm with Censored Data: A Case Study on Centrifugal Pumps in an Oil Refinery,” 2023.

[43] A. Patil, S. Sundar, A. Delgado, and J. Gamboa, “CFD based evaluation of conventional electrical submersible pump for high-speed application,” *J. Pet. Sci. Eng.*, vol. 182, p. 106287, 2019.

[44] S. Chakraborty, K. Choudhuri, P. Dutta, and B. Debbarma, “Performance prediction of Centrifugal Pumps with variations of blade number,” 2013.

[45] Y. Liu, L. Tan, Y. Hao, and Y. Xu, “Energy performance and flow patterns of a mixed-flow pump with different tip clearance sizes,” *Energies*, vol. 10, no. 2, p. 191, 2017.

[46] F. Kenyery, “Effect of Bubble Size on an ESP Performance Handling Two-Phase Flow Conditions.”

[47] M. Murakami and K. Minemura, “Flow of air bubbles in centrifugal impellers and its effect on the pump performance,” in *Proc. 6th Australasian Hydraulics and Fluid Mechanics Conf*, 1977, vol. 1, pp. 382–385.

[48] G. R. Noghrehkar, M. Kawaji, A. M. C. Chan, H. Nakamura, and Y. Kukita, “Investigation of centrifugal pump performance under two-phase flow conditions,” 1995.

[49] J. Zhu and H.-Q. Zhang, “CFD simulation of ESP performance and bubble size estimation under gassy conditions,” in *SPE Annual Technical Conference and Exhibition?*, 2014, p. SPE-170727.

[50] Y. Lin, T. Fan, and X. Zheng, “Roles of recirculating bubble on the performance of centrifugal compressors,” *Aerosp. Sci. Technol.*, vol. 118, p. 107073, 2021.

[51] J. Zhu and H.-Q. Zhang, “Numerical study on electrical-submersible-pump two-phase performance and bubble-size modeling,” *SPE Prod. Oper.*, vol. 32, no. 03, pp. 267–278, 2017.

[52] Q. Si, W. He, G. Bois, Q. Cui, S. Yuan, and K. Zhang, “Experimental and numerical studies on flow characteristics of centrifugal pump under air-water inflow,” *Int. J. Fluid Mach. Syst.*, vol. 12, no. 1, pp. 31–38, 2019.

[53] A. A. Kulkarni and J. B. Joshi, “Bubble formation and bubble rise velocity in gas−liquid systems: a review,” *Ind. Eng. Chem. Res.*, vol. 44, no. 16, pp. 5873–5931, 2005.

[54] J. Zhu *et al.*, “Modeling flow pattern transitions in electrical submersible pump under gassy flow conditions,” *J. Pet. Sci. Eng.*, vol. 180, pp. 471–484, 2019.

[55] A. Amoresano, G. Langella, and C. Noviello, “Experimental analysis of air bubble inside a centrifugal pump,” *WIT Trans. Modelling Simul.*, vol. 30, 2001.

[56] A. Ali *et al.*, “Research progress and prospects of multi-stage centrifugal pump capability for handling gas–liquid multiphase flow: Comparison and empirical model validation,” *Energies*, vol. 14, no. 4, p. 896, 2021.

[57] L. Barrios and M. G. Prado, “Experimental visualization of two-phase flow inside an electrical submersible pump stage,” 2011.

[58] W. M. Verde, J. L. Biazussi, N. A. Sassim, and A. C. Bannwart, “Experimental study of gas-liquid two-phase flow patterns within centrifugal pumps impellers,” *Exp. Therm. Fluid Sci.*, vol. 85, pp. 37–51, 2017.

[59] J. M. C. Cubas, H. Stel, E. M. Ofuchi, M. A. M. Neto, and R. E. M. Morales, “Visualization of two-phase gas-liquid flow in a radial centrifugal pump with a vaned diffuser,” *J. Pet. Sci. Eng.*, vol. 187, p. 106848, 2020.

[60] J. Caridad, M. Asuaje, F. Kenyery, A. Tremante, and O. Aguillón, “Characterization of a centrifugal pump impeller under two-phase flow conditions,” *J. Pet. Sci. Eng.*, vol. 63, no. 1–4, pp. 18–22, 2008.

[61] W. Zhang, Z. Yu, and Y. Li, “Application of a non-uniform bubble model in a multiphase rotodynamic pump,” *J. Pet. Sci. Eng.*, vol. 173, pp. 1316–1322, 2019.

[62] H. Pineda *et al.*, “Phase distribution analysis in an Electrical Submersible Pump (ESP) inlet handling water–air two-phase flow using Computational Fluid Dynamics (CFD),” *J. Pet. Sci. Eng.*, vol. 139, pp. 49–61, 2016.

[63] G. Shi, H. Li, X. Liu, Z. Liu, and B. Wang, “Transport performance improvement of a multiphase pump for gas–liquid mixture based on the orthogonal test method,” *Processes*, vol. 9, no. 8, p. 1402, 2021.

[64] A. Hasan, S. Shahid, S. S. Dol, M. S. Gadala, M. S. Aris, and M. Alavi, "Effects of Rotation Speeds on Electrical Submersible Pump Performance Under Two-Phase Flow," in *Intelligent Manufacturing and Energy Sustainability: Proceedings of ICIMES 2021*, 2022, pp. 599–608.

[65] H. K. Versteeg and W. Malalasekera, *An introduction to computational fluid dynamics: the finite volume method*. Pearson education, 2007.

[66] T. Norton, B. Tiwari, and D.-W. Sun, "Computational fluid dynamics in the design and analysis of thermal processes: a review of recent advances," *Crit. Rev. Food Sci. Nutr.*, vol. 53, no. 3, pp. 251–275, 2013.

[67] D. C. Wilcox, "Turbulence modeling for CFD. La Canada, CA: DCW Industries," *Inc, Novemb.*, vol. 34, 2006.

[68] J. H. Ferziger, M. Perić, and R. L. Street, *Computational methods for fluid dynamics*. springer, 2019.

[69] R. W. Erney, "Verification and validation of single phase and cavitating flows using an open source CFD tool," 2009.

[70] C. Vallée, T. Höhne, H.-M. Prasser, and T. Sühnel, "Experimental investigation and CFD simulation of horizontal stratified two-phase flow phenomena," *Nucl. Eng. Des.*, vol. 238, no. 3, pp. 637–646, 2008.

[71] I. Ansys, "Fluent theory guide," *ANSYS Inc, USA [(accessed 27 March 2020)]*, 2013.

[72] J. Majdalani, "A special collection to celebrate the life of Professor Frank M. White," *Phys. Fluids*, vol. 34, no. 9, 2022.

[73] S. B. Pope, *Turbulent flows*. Cambridge university press, 2000.

[74] B. E. Launder and B. I. Sharma, "Application of the energy-dissipation model of turbulence to the calculation of flow near a spinning disc," *Lett. heat mass Transf.*, vol. 1, no. 2, pp. 131–137, 1974.

[75] L. Schiller, “A drag coefficient correlation,” *Zeit. Ver. Deutsch. Ing.*, vol. 77, pp. 318–320, 1933.

[76] R. Clift, J. R. Grace, and M. E. Weber, “Bubbles, drops, and particles,” 2005.

[77] M. C. Roco, “Particulate two-phase flow,” *(No Title)*, 1993.

[78] D. Legendre and J. Magnaudet, “The lift force on a spherical bubble in a viscous linear shear flow,” *J. Fluid Mech.*, vol. 368, pp. 81–126, 1998.

[79] A. Fluent, “ANSYS fluent theory guide 15.0,” *ANSYS, Canonsburg, PA*, vol. 33, 2013.

[80] D. J. Añez, F. Kenyery, S. I. Escalante, and V. M. Teran, “ESP’s Performance With Two Phase and Viscous Flow,” in *Engineering Technology Conference on Energy*, 2001, vol. 80203, pp. 795–799.

[81] G. Shi, S. Tao, X. Liu, H. Wen, and Z. Shu, “Effect of gas volume fraction on the gas-phase distribution in the passage and blade surface of the axial flow screw-type oil-gas multiphase pump,” *Processes*, vol. 9, no. 5, p. 760, 2021.